Metric based up-scaling

Houman Owhadi*and Lei Zhang†

November 15, 2005

Abstract

We consider divergence form elliptic operators in dimension $n \geq 2$ with L^∞ coefficients. Although solutions of these operators are only Hölder continuous, we show that they are differentiable ($C^{1,\alpha}$) with respect to harmonic coordinates. It follows that numerical homogenization can be extended to situations where the medium has no ergodicity at small scales and is characterized by a continuum of scales by transferring a new metric in addition to traditional averaged (homogenized) quantities from subgrid scales into computational scales and error bounds can be given. This numerical homogenization method can also be used as a compression tool for differential operators.

1 Introduction and main results

Let Ω be a bounded and convex domain of class C^2. We consider the following benchmark PDE

$$\begin{cases} -\operatorname{div}\left(a(x)\nabla u(x)\right) = g \quad \text{in} \quad \Omega \\ u = 0 \quad \text{in} \quad \partial\Omega. \end{cases} \tag{1.1}$$

Where g is a function in $L^\infty(\Omega)$. And $x \to a(x)$ is a mapping from Ω into the space of positive definite symmetric matrices. We assume a to be symmetric, uniformly elliptic with entries in $L^\infty(\Omega)$.

AMS 1991 *Subject Classification.* Primary 34E13,35B27 ; secondary 68P30, 60F05, 35B05.

Key words and phrases. Multi scale problem, compensation, homogenization, multi-fractal, numerical homogenization, compression.

*California Institute of Technology Applied & Computational Mathematics, Control & Dynamical systems, MC 217-50 Pasadena , CA 91125, owhadi@caltech.edu

†California Institute of Technology Applied & Computational Mathematics MC 217-50 Pasadena , CA 91125, zhanglei@acm.caltech.edu

- Is it possible to up-scale (1.1)?

Homogenization theory ([15], [52]) allows us to do so by transferring bulk (averaged) information from sub-grid scales into computational scales. This transfer from a numerical homogenization point of view is justified under two fundamental assumptions:

- Ergodicity at small scales, and
- scale separation.

Can we get rid of these assumptions?

- Can we numerically homogenize (1.1) when a is arbitrary? in particular when a is characterized by a continuum of scales with no ergodicity at small scales?

What do we mean by numerical homogenization when a is arbitrary? It is important to recall that F. Murat and L. Tartar's theory of H-convergence [61] provides a mathematical framework for analysis of composites in complete generality, without any need for geometrical hypotheses such as periodicity or randomness. This theory is based on a powerful tool called compensated compactness or div-curl lemma introduced in the 70's by Murat and Tartar [60], [73] which has been characterized by a wide range of applications and refinements [25]. Here we consider homogenization from a slightly different point of view: we want to solve (1.1) on a coarse mesh and we want to understand which information should be transferred from fine scales to coarse scales when the entries of a are arbitrary. For that purpose we need a new form of compensation given in section 1.1.

It is important to observe that if one needs to solve (1.1) only one time (with one g) the method proposed here does not reduce the number of numerical operations[1]. Indeed we need to compute (1.1) n-times (n being the space dimension) with 0 in the right hand side in (1.1) and linear boundary conditions. However if one needs to solve (1.1) for a large number (M) of different right hand sides g ($M >> n$, which would happen if one tries to optimize specific properties of u with respect to g) then the methods proposed here have a practical use since they basically say that after solving (1.1) n times it is sufficient to solve (1.1) on a coarse mesh (with $N^{0.01}$ nodes instead of N for instance) M times.

Let us recall that fast methods based on hierarchical matrices are available [13, 9, 12, 10, 11] for solving (1.1) in $O\big(N(\ln N)^{n+3}\big)$ operations.

Finally the point of view of this paper is to observe the "redundancy" of solutions of (1.1) at small scales rather than "fast computation". Indeed it is not obvious that (1.1) can be homogenized when the medium does

[1]It will be shown in [65] that for parabolic and reaction-diffusion equations the situation is different: the methodology introduced in this paper can be used to reduce the number of operations even when one needs to solve these equations only once.

not satisfy the usual periodicity, ergodicity or scale-separation assumptions. Moreover if (1.1) can indeed be homogenized it is important to understand what minimal quantity of information should be kept from small scales to obtain an accurate homogenized operator? Once the correct coarse parameters are identified (the bulk quantities and the up-scaled metric), one can try to model, estimate or simulate them but the first step is to identify them.

1.1 A new form of compensation

To introduce the new form of compensation, we need to introduce the so called a-harmonic coordinates associated to (1.1), i.e. the weak solution of the following boundary value problem

$$\begin{cases} \operatorname{div} a\nabla F = 0 \quad \text{in} \quad \Omega \\ F(x) = x \quad \text{on} \quad \partial\Omega. \end{cases} \tag{1.2}$$

By (1.2) we mean that F is a n-dimensional vector field $F(x) = \big(F_1(x), \dots, F_n(x)\big)$ such that each of its entries satisfies

$$\begin{cases} \operatorname{div} a\nabla F_i = 0 \quad \text{in} \quad \Omega \\ F_i(x) = x_i \quad \text{on} \quad \partial\Omega. \end{cases} \tag{1.3}$$

The new compensation phenomenon is controlled by the following object:

Definition 1.1. We write

$$\sigma := {}^t\nabla F a \nabla F. \tag{1.4}$$

We write μ_σ the anisotropic distortion of σ defined by

$$\mu_\sigma := \operatorname{esssup}_{x\in\Omega}\Big(\frac{\lambda_{\max}\big(\sigma(x)\big)}{\lambda_{\min}\big(\sigma(x)\big)}\Big). \tag{1.5}$$

Where $\lambda_{\max}(M)$ ($\lambda_{\min}(M)$) denote the maximal (minimal) eigenvalue of M.

Definition 1.2. In dimension $n = 2$, we say that σ *is stable if and only if* $\mu_\sigma < \infty$ *and there exist a constant* $\epsilon > 0$ *such that* $\big(\operatorname{Trace}(\sigma)\big)^{-1-\epsilon} \in L^1(\Omega)$

Remark 1.1. According to [4] in dimension two if a is smooth then σ is stable. According to [1], F is always an homeomorphism in dimension two even with $a_{i,j} \in L^\infty(\Omega)$.

Theorem 1.1. *Assume that* σ *is stable and* $n = 2$. *Then there exist constants* $\alpha > 0$ *and* $C > 0$ *such that* $(\nabla F)^{-1}\nabla u \in C^\alpha(\Omega)$ *and*

$$\big\|(\nabla F)^{-1}\nabla u\big\|_{C^\alpha(\Omega)} \leq C\|g\|_{L^\infty(\Omega)}. \tag{1.6}$$

Remark 1.2. The constant α depends on $\Omega, \lambda_{\max}(a)/\lambda_{\min}(a)$ and μ_σ. The constant C depends on the constants above, $\lambda_{\min}(a)$ and $\big\|\big(\operatorname{Trace}(\sigma)\big)^{-1-\epsilon}\big\|_{L^1(\Omega)}$. We use the notation $\lambda_{\max}(a) := \sup_{x\in\Omega}\sup_{|\xi|=1} {}^t\xi a\xi$ and $\lambda_{\max}(a) := \inf_{x\in\Omega}\inf_{|\xi|=1} {}^t\xi a\xi$.

Remark 1.3. If one considers a sequence a_ϵ such that μ_{σ_ϵ} and $\big\|\big(\operatorname{Trace}(\sigma_\epsilon)\big)^{-1-\epsilon}\big\|_{L^1(\Omega)}$ are uniformly bounded away from ∞ and $\lambda_{\min}(a_\epsilon)$ and $\lambda_{\max}(a_\epsilon)$ are uniformly bounded away from 0 and ∞ then (1.6) is uniformly true. If we consider a periodically oscillating sequence $a_\epsilon(x) = a(\frac{x}{\epsilon})$, $\mu_{\sigma_1} < \infty$ and $\big\|\big(\operatorname{Trace}(\sigma_1)\big)^{-1-\epsilon}\big\|_{L^1(\Omega)} < \infty$ then (1.6) is uniformly true.

Remark 1.4. It is easy to check from the proof of 1.1 that if $\big(\operatorname{Trace}(\sigma_\epsilon)\big)^{-1} \in L^q(\Omega)$ (with $q > 2$) then it is possible to replace $\|g\|_{L^\infty(\Omega)}$ by $\|g\|_{L^p(\Omega)}$ in (1.6) with p depending on q. More precisely if $\big(\operatorname{Trace}(\sigma_\epsilon)\big)^{-1} \in L^\infty(\Omega)$ then it is possible to replace $\|g\|_{L^\infty(\Omega)}$ by $\|g\|_{L^{2+\epsilon}(\Omega)}$ in (1.6) for any $\epsilon > 0$.

Remark 1.5. We don't need a to be symmetric to obtain 1.1 but for the clarity of the presentation we have chosen to restrict ourselves to that case. We have not analyzed Neumann boundary conditions, this will done in a further work.

Remark 1.6. We will use the notation $\nabla_F u := (\nabla F)^{-1}\nabla u$. In dimension two, it is known ([4], [6], [1]) that the determinant of ∇F is strictly positive almost everywhere and the object $\nabla_F u$ is well defined. In dimension three and higher $\nabla_F u$ is well defined when σ is stable.

This phenomenon can be observed numerically. In figures 1(a) and 2(a) a is given by a product of random functions oscillating over a continuum of scales. The entries of the matrix ∇F are in L^p (figure 2(b)), the entries of the gradient of u in the Euclidean metric are in L^p (figures 1(b) and 2(c)) yet $(\nabla F)^{-1}\nabla u$ is Hölder continuous (figures 1(c) and 2(d)).

Let us now introduce the compensation phenomenon in dimension $n \geq 3$. We call β_σ the Cordes parameter associated to σ defined by

$$\beta_\sigma := \operatorname{esssup}_{x\in\Omega}\Big(n - \frac{\big(\operatorname{Trace}[\sigma(x)]\big)^2}{\operatorname{Trace}[{}^t\sigma(x)\sigma(x)]}\Big). \tag{1.7}$$

Observe that since β_σ is also given by

$$\beta_\sigma = \operatorname{esssup}_{x\in\Omega}\Big(n - \frac{\big(\sum_{i=1}^n \lambda_{i,\sigma(x)}\big)^2}{\sum_{i=1}^n \lambda_{i,\sigma(x)}^2}\Big). \tag{1.8}$$

where $(\lambda_{i,M})$ denotes the eigenvalues of M, it is a measure of the anisotropy of σ.

Definition 1.3. In dimension $n \geq 3$, we say that σ is stable if and only if, $\beta_\sigma < 1$ and if $n \leq 4$ that there exist a constant $\epsilon > 0$ such that $\big(\operatorname{Trace}(\sigma)\big)^{\frac{n}{2}-2-\epsilon} \in L^1(\Omega)$

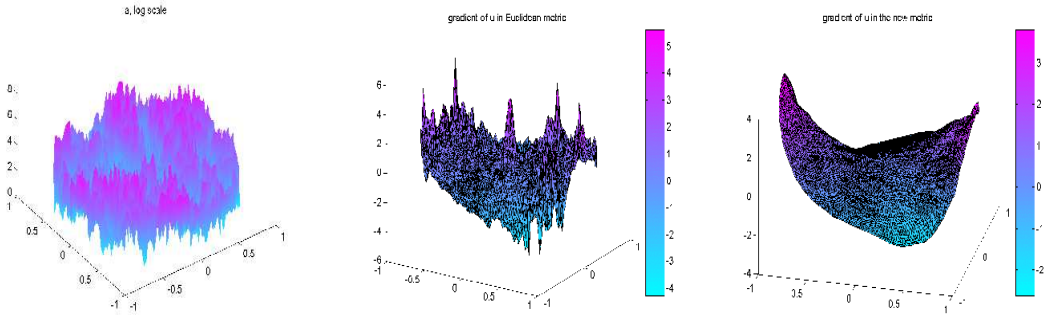

(a) a ***in log scale.*** **(b)** ∇u**.** **(c)** $(\nabla F)^{-1}\nabla u$**.**

Figure 1: Change of metric on the disk.

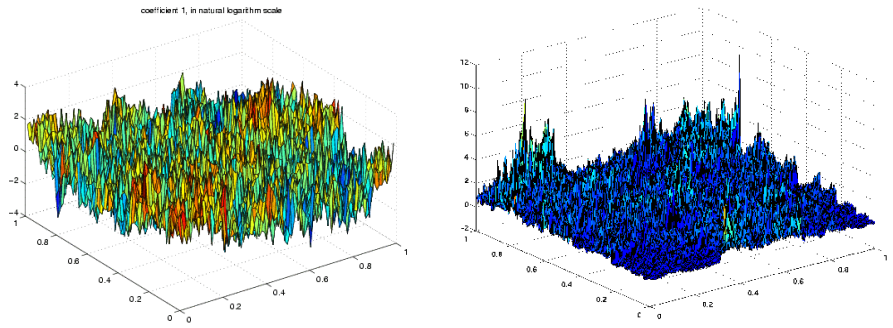

(a) a ***in log scale.*** **(b)** ***one of the entries*** ∇F**.**

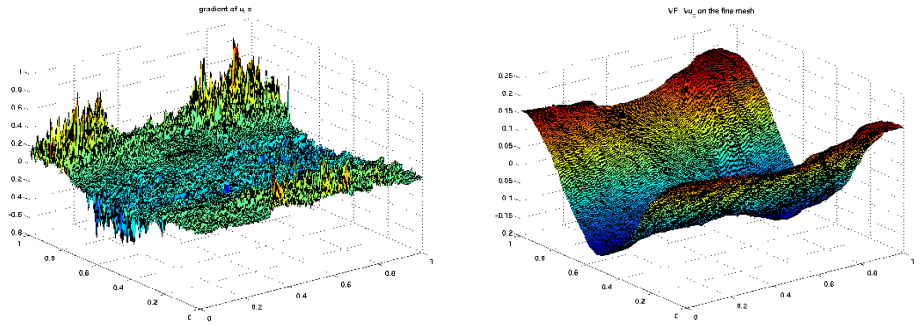

(c) ∇u**.** **(d)** $(\nabla F)^{-1}\nabla u$**.**

Figure 2: Change of metric on the torus.

Remark 1.7. According to [4] and [21] in dimension three and higher σ can be unstable even if a is smooth. We refer to figure 6 for an explicit example.

Let us write

$$\|v\|_{W_0^{2,p}(\Omega)} := \Big(\int_\Omega \big(\sum_{i,j=1}^n |\partial_i \partial_j v|^2 \big)^{\frac{p}{2}} \, dx \Big)^{\frac{1}{p}} \tag{1.9}$$

Theorem 1.2. *Assume that σ is stable and $n \geq 3$. Then F is an automorphism on Ω. Moreover there exist constants $p > 2$ and $C > 0$ such that $u \circ F^{-1} \in W_0^{2,p}(\Omega)$ and*

$$\big\| u \circ F^{-1} \big\|_{W_0^{2,p}(\Omega)} \leq C \|g\|_{L^\infty(\Omega)}. \tag{1.10}$$

Remark 1.8. The constant p depends on n, Ω and β_σ. The constant C depends on the constants above, $\lambda_{\min}(a)$ and if $n \leq 4$ on $\big\| \big(\operatorname{Trace}(\sigma) \big)^{\frac{n}{2}-2-\epsilon} \big\|_{L^1(\Omega)}$.

In the following theorem we do not need to assume Ω to be convex.

Theorem 1.3. *Assume $n \geq 2$ and $(\operatorname{Trace}(\sigma))^{-1} \in L^\infty(\Omega)$. Let $p > 2$. There exist a constant $C^* = C^*(n, \partial\Omega) > 0$ such that if $\beta_\sigma < C^*$ then there exists a real number $\gamma > 0$ depending only on n, Ω and p such that*

$$\big\| (\nabla F)^{-1} \nabla u \big\|^2_{C^\gamma(\Omega)} \, dt \leq C \|g\|^2_{L^p(\Omega)}. \tag{1.11}$$

Remark 1.9. The constant C in (1.11) depends on n, γ, Ω, C^*, $\lambda_{\min}(a)$, $\|a\|_{L^\infty(\Omega)}$, μ_σ and $\big\| (\operatorname{Trace}(\sigma))^{-1} \big\|_{L^\infty(\Omega_T)}$.

1.2 Dimensionality reduction

Observe that (1.1) is a priori an infinite dimensional problem since a and g can be irregular at all scales. Yet according to theorem 1.1 and 1.2, whatever the choice of g, at small scales, solutions to (1.1) are correlated to F which lives in a functional space of dimension n. More precisely we will propose a rigorous justification of a variation of the multi-scale finite element method[2] introduced by Hou and Wu [49] in its form refined by Allaire and Brizzi [2] in situations where the medium is not assumed to be periodic or ergodic (these methods are already rigorously justified when the medium is periodic [49], [2]).

Let $\mathcal{T}_h$ be a coarse conformal mesh on Ω composed of n-simplices(triangles in dimension two and tetrahedra in dimension three). Here h is the usual resolution of the mesh defined as the maximal length of the edges of the tessellation. Let us call $\gamma(\mathcal{T}_h)$ the maximum over of the n-simplices K of $\mathcal{T}_h$

[2]Let us recall that the multi-scale finite element method is inspired from Tartar's oscillating test functions [74]

of the ratio between the radius of the smallest ball containing K and the largest ball inscribed in K. We assume $\gamma(\mathcal{T}_h)$ to be uniformly bounded in h.

We write $V_h \subset H^1(\Omega)$ the set of piecewise linear functions on the coarse mesh vanishing at the boundary of the tessellation. We write $\mathcal{N}_h$ the set of interior nodes of the tessellation and φ_i ($i \in \mathcal{N}_h$) the usual nodal basis function of V_h satisfying

$$\varphi_i(y_j) = \delta_{ij}. \tag{1.12}$$

We consider the elements $(\psi_i)_{i\in\mathcal{N}_h}$ defined by

$$\psi_i := \varphi_i \circ F(x). \tag{1.13}$$

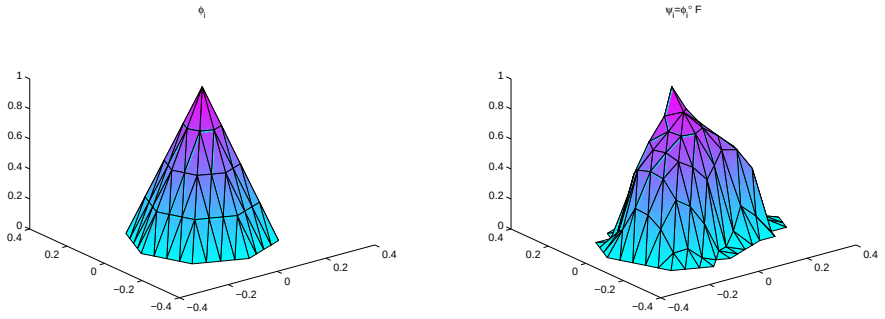

(a) φ_i **(b)** $\psi_i = \varphi_i \circ F$

Figure 3: The Galerkin elements

Let us write u_h the solution of the Galerkin scheme associated to (1.2) based on the elements $(\psi_i)_{i\in\mathcal{N}_h}$. Observe that the number of elements is on the order of h^{-n} and we have the following theorem

Theorem 1.4. *Assume that σ is stable and $n = 2$. Then there exist constants $\alpha, C > 0$ such that*

$$\|u - u_h\|_{H^1} \leq Ch^\alpha \|g\|_{L^\infty(\Omega)}. \tag{1.14}$$

Remark 1.10. The constant α depends only on n, Ω and μ_σ. The constant C depends on the objects mentioned above plus $\lambda_{\min}(a), \lambda_{\max}(a)$, $\gamma(\mathcal{T}_h)$ and $\left\| \big(\operatorname{Trace}(\sigma) \big)^{-1-\epsilon} \right\|_{L^1(\Omega)}$.

Remark 1.11. Theorem 1.4 is also valid with $\alpha = 1$ as in theorem 1.5. The only difference between these two theorems lies in the constant C. In the proof theorem 1.4 we use the property $u \circ F^{-1} \in C^{1,\alpha}(\Omega)$ and in the proof of theorem 1.5 we use the property $u \circ F^{-1} \in W^{2,2}(\Omega)$.

Remark 1.12. Let us recall that u_h is an element of the space X_h spanned by $(\psi_i)_{i\in\mathcal{N}_h}$ obtained as the solution of the linear problem

$$a[\psi_i, u_h] = (\psi_i, g)_{L^2(\Omega)}. \tag{1.15}$$

Where $a[,]$ is the bilinear form on $H^1_0(\Omega)$ defined by

$$a[v, w] := \int_\Omega \nabla v a \nabla w. \tag{1.16}$$

It follows from theorem 1.4 that solutions to (1.1) live in the H^1-norm neighborhood of a low dimensional space.

Remark 1.13. The proof of theorem 1.4 is done for the exact function ψ_i and not for its discrete version on a fine mesh. If a is regular at a given small scale h_0 then it is easy to check that theorem 1.4 remains valid as long as the edges of the fine mesh are smaller than h_0. A more intriguing case is when a is discrete and discontinuous on a fine mesh. Numerical experiments show that theorems such as 1.4 and 1.1 remain valid but to justify them for the discrete version of the harmonic coordinates F and elements ψ_i one would have to adapt our theorems to the discrete setting. In order to remain concise we have chosen to not include that adaptation in this paper.

Remark 1.14. We keep the composition rule used in [2]. The only difference between the elements (1.13) and the ones proposed by Hou, Wu, Allaire and Brizzi lies in the fact that we use the global solution to (1.2) and not a local one computed on each triangle of the coarse mesh through an over-sampling technique. We refer to remark 3.1 for further comments.

Remark 1.15. Write S the stiffness matrix $a[\psi_i, \psi_j]$. S^{-1} is in general dense (characterized by N^2 entries where N is the number of nodes of the mesh). Yet surprisingly by combining theorem 1.4 with theorem 5.4 of [13] one can obtain that S^{-1} can be approximated (in L^2 norm) with hierarchical matrix M_H such that the matrix vector product by M_H requires only $O(N(\ln N)^{n+3})$ operations.

In dimension $n \geq 3$ we have the following estimate.

Theorem 1.5. *Assume that σ is stable, $n \geq 3$ and $\left\| \left(\operatorname{Trace}(\sigma) \right)^{-1} \right\|_{L^\infty(\Omega)} < \infty$. Then there exist constants $\alpha, C > 0$ such that*

$$\|u - u_h\|_{H^1} \leq Ch\|g\|_{L^\infty(\Omega)}. \tag{1.17}$$

Remark 1.16. The constant C depends on n, $\gamma(\mathcal{T}_h)$, Ω, β_σ, $\lambda_{\max}(a)$, $\lambda_{\min}(a)$ and $\left\| \left(\operatorname{Trace}(\sigma) \right)^{-1} \right\|_{L^\infty(\Omega)}$.

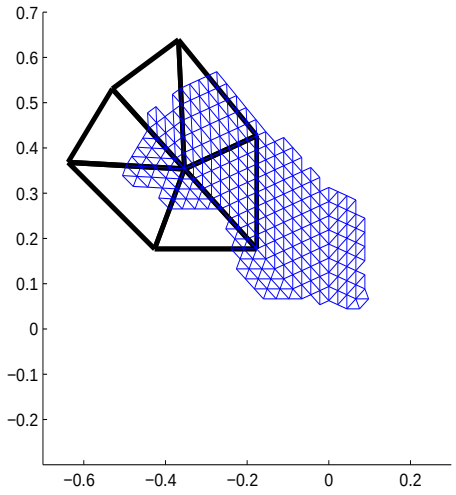

Figure 4: Support of the elements φ_i and ψ_i.

1.3 Galerkin with localized elements

For the clarity of the paper we will restrict ourselves from now on to dimension two, the generalization of the statements to higher dimensions is conditioned on the stability of σ (and the application of theorem 1.3).

The elements (1.13) can be highly distorted and non local (figure 4) since

$$\text{support}(\psi_i) := F^{-1}\big(\text{support}(\varphi_i)\big). \tag{1.18}$$

It follows that the elements ψ_i are piecewise linear on a fine mesh different from the one on which a is defined and F has been computed. Is it possible to avoid that difficulty by solving (1.1) on a coarse mesh with localized elements? The answer is yes but the price to pay for the localization will be the discontinuity of the elements and the fact that the accuracy of the method will depend on a weak aspect ratio of the triangles of the tessellation in the metric induced by F. More precisely consider a triangle K of the tessellation, call a, b, c the nodes of K and θ the interior angle of the triangle $\big(F(a), F(b), F(c)\big)$ which is the closest to $\pi/2$. We call weak aspect ratio of the triangle K in the metric induced by F the quantity

$$\eta^F_{\min}(K) := \frac{1}{\sin(\theta)}. \tag{1.19}$$

So $\eta^F_{\min}(K)$ is large if the triangle $\big(F(a), F(b), F(c)\big)$ is flat (all its interior

angles are close to 0 or π). We define

$$\eta^*_{\min} := \sup_{K\in\mathcal{T}_h} \eta^F_{\min}(K). \tag{1.20}$$

Let us recall that although the coefficients of the PDE (1.1) are irregular it is well known [70] that F is Hölder continuous. Thus it makes sense to look at the value of F at a specific point. Now let v be a function defined on the nodes of the triangle $K \in \mathcal{T}_h$, let us write a, b, c the nodes of that triangle. It is usual to look at the coarse gradient of v evaluated at the nodes of the triangle K, i.e. the vector defined by

$$\nabla v(K) := \begin{pmatrix} b-a \\ c-a \end{pmatrix}^{-1} \begin{pmatrix} v(b)-v(a) \\ v(c)-v(a) \end{pmatrix}. \tag{1.21}$$

If $\eta^F_{\min}(K) < \infty$ then the following object called the gradient of v evaluated on the coarse mesh with respect to the metric induced by F is well defined.

$$\nabla_F v(K) := \begin{pmatrix} F(b)-F(a) \\ F(c)-F(a) \end{pmatrix}^{-1} \begin{pmatrix} v(b)-v(a) \\ v(c)-v(a) \end{pmatrix}. \tag{1.22}$$

Definition 1.4. We say that the tessellation $\mathcal{T}_h$ is not unadapted to F if and only if the determinant of $\nabla F(K)$ is strictly positive for all $K \in \mathcal{T}_h$.

Remark 1.17. Observe that if the tessellation $\mathcal{T}_h$ is not unadapted to F then $\eta^*_{\min}(K) < \infty$, the definition 1.4 contains the additional condition that there is no inversion in the images of the triangles of $\mathcal{T}_h$ by F.

Now consider the nodal elements $(\xi_i)_{i\in\mathcal{N}_h}$, defined by

$$\begin{cases} \xi_i(x_j) = \delta_{ij} \\ \nabla_F \xi(x) = \text{constant within each} \quad K \in \mathcal{T}_h. \end{cases} \tag{1.23}$$

If the mesh is not unadapted to F then the elements (figure 5) (1.23) are well defined and given by

$$\begin{cases} \xi_i(x) = 1 + \big(F(x) - F(x_i)\big)\nabla_F \varphi_i(K) \quad \text{if} \quad i \sim K \quad \text{and} \quad x \in K \\ \xi_i(0) = 0 \quad \text{in other cases.} \end{cases} \tag{1.24}$$

Where the notation $i \sim K$ means that i is a node of K. Observe that the elements ξ_i are discontinuous at the boundaries of the triangles of the coarse mesh however they are easier to implement since they are localized in these triangles. Write Z_h the vector space spanned by the functions ξ_i. For $K \in \mathcal{T}_h$ we write a_K the bilinear form on $H^1(K)$ defined by

$$a_K[v, w] := \int_K {}^t\nabla v a \nabla w. \tag{1.25}$$

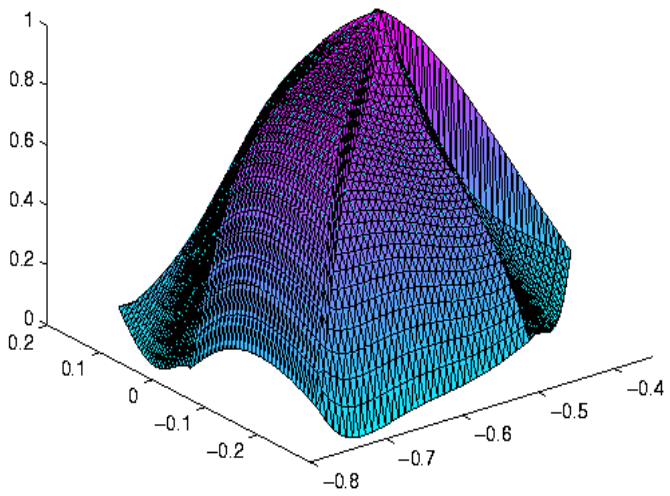

Figure 5: Localized Galerkin elements ξ_i

We will write $H^1(\mathcal{T}_h)$ the space of functions $v \in L^2(\Omega)$ such that the restriction of v to each triangle K belongs to $H^1(K)$. We will write for $v, w \in H^1(\mathcal{T}_h)$

$$a^*[v,w] := \sum_{K\in\mathcal{T}_h} a_K[v,w]. \tag{1.26}$$

The localized finite element method can be formulated in the following way: look for $u^f \in Z_h$ such that for all $i \in \mathcal{N}_h$,

$$a^*[\xi_i, u^f] = (\xi_i, g)_{L^2(\Omega)}. \tag{1.27}$$

We have the following estimate

Theorem 1.6. *Assume that σ is stable and that the mesh is not unadapted to F. Then there exists a constant $\alpha > 0$ such that*

$$\big(a^*[u-u^f]\big)^{\frac{1}{2}} \leq C\eta^*_{\min} h^\alpha \|g\|_{L^\infty(\Omega)}. \tag{1.28}$$

Remark 1.18. For a bilinear from $B[,]$ we write $B[v] := B[v,v]$.

Remark 1.19. The constant α depends only on n, Ω, ϵ and μ_σ. The constant C depends on the objects mentioned above plus $\big\|\big(\operatorname{Trace}(\sigma)\big)^{-1-\epsilon}\big\|_{L^1(\Omega)}$.

Remark 1.20. The bilinear operator $a^*[,]$ on Z_h is characterized by a constant matrix within each triangle $K \in \mathcal{T}_h$ equal to

$$ {}^t\big(\nabla F(K)\big)^{-1}\big\langle {}^t\nabla F a \nabla F\big\rangle_K\big(\nabla F(K)\big) \tag{1.29}$$

where $< v >_K$ means the average of v over K with respect to the Lebesgue measure ($< v >_K := \frac{1}{\mathrm{Vol}(K)} \int_K v(x)\,dx$, $\mathrm{Vol}(K)$ being the Lebesgue measure of volume of K).

The error bound given in theorem 1.6 is given in the norm induced by $a^*[.]$. We would like to obtain an error bound with respect to the usual H^1 norm. Observe that u^f is discontinuous at the boundaries of the triangles of the coarse mesh so we have to find an accurate way to interpolate u^f in the whole space using its values at the nodes of the coarse mesh. Let us write $F(\mathcal{N}_h)$ the image of the nodes of $\mathcal{T}_h$ by F. Let us write $\mathcal{T}^F$ the triangulation of $F(\mathcal{N}_h)$. Let φ_i^F be the standard piecewise linear nodal basis of $\mathcal{T}^F$. Let us write $\mathcal{J}_h$ the interpolation operator from the space of functions defined on the nodes of $\mathcal{T}_h$ into $H^1(\Omega)$ defined by

$$ \mathcal{J}_h v(x) := \sum_{i \in \mathcal{N}_h} v(x_i)\varphi_i^F \circ F(x). \tag{1.30}$$

Observe that for $i \in \mathcal{N}_h$, $v(x_i) = \mathcal{J}_h v(x_i)$. We have the following estimate

Theorem 1.7. *Assume that σ is stable and that the mesh is not unadapted to F. Then there exist constants $\alpha, C_f > 0$ such that*

$$ \|u - \mathcal{J}_h u^f\|_{H^1(\Omega)} \leq C_f h^\alpha \|g\|_{L^\infty(\Omega)}. \tag{1.31}$$

Remark 1.21. The constant α depends only on n, Ω and μ_σ. The constant C_f can be written

$$ C_f := C\eta_{\min}^* \Big(\min\big(\eta_{\max}^* \eta_{\max}^3, \nu^*\big)\Big)^{\frac{1}{2}} \tag{1.32}$$

where C depends on the objects mentioned above plus $\lambda_{\min}(a), \lambda_{\max}(a)$ and $\big\|\big(\mathrm{Trace}(\sigma)\big)^{-1-\epsilon}\big\|_{L^1(\Omega)}$. $\eta_{\max}$ is defined by $\frac{1}{\sin\theta}$ where θ the interior angle of the triangles of $\mathcal{T}_h$ closest to 0 or π. $\eta_{\max}^*$ is defined by $\frac{1}{\sin\gamma}$ where γ the interior angle of the triangles of $\mathcal{T}^F$ closest to 0 or π. Moreover

$$ \nu^* := \sup_{K \in \mathcal{T}_h} \frac{\mathrm{Vol}(K^F)}{\mathrm{Vol}(F(K))} \tag{1.33}$$

where K^F is the triangle whose nodes are the images of the nodes of K by F.

1.4 Numerical homogenization from the information point of view.

The Galerkin scheme described in 1.2 and 1.3 are based on elements containing the whole fine scale structure of F. This represents too much information. We can wonder what minimal quantity of information should be kept from the scales in order to up-scale (1.1)? We would like to keep an accurate version of (1.1) with minimal computer memory. This point touches the compression issue. Images can be compressed. Can the same thing be done with operators?

This question has received an answer within the context of the fast multiplication of vectors with fully populated special matrices arising in various applications [35]. Let us recall the fast multipole method and the hierarchical multipole method designed by L. Greengard and V. Rokhlin [43]. Wavelet based methods have been designed by G. Beylkin, R. Coifman and V. Rokhlin [3, 17, 16]. The concept of Hierarchical matrices has been developed by W. Hackbusch et al. [45]. More precisely we refer to [13, 9, 12, 10, 11]. The Hierarchical matrix method is based on a compression of the inverse of the stiffness matrix (see remark 1.15). Here we consider compression from the point of view of numerical homogenization. We look at the operator (1.1) as a bilinear form on $H_0^1(\Omega)$ and we will use V_h as space of test functions to *zoom at* the operator associated to a at a given arbitrary resolution.

$$a : \begin{cases} H_0^1(\Omega) \times H_0^1(\Omega) & \to \mathbb{R} \\ (v, w) & \to \int_\Omega {}^t\nabla v a \nabla w. \end{cases} \tag{1.34}$$

The up-scaled or compressed operator, written $\mathcal{U}_h a$ will naturally be a bilinear form on the space of piecewise linear functions on the coarse mesh with Dirichlet boundary condition.

$$\mathcal{U}_h a : \begin{cases} V_h \times V_h & \to \mathbb{R} \\ (v, w) & \to \mathcal{U}_h a[v, w]. \end{cases} \tag{1.35}$$

The question is how to choose $\mathcal{U}_h a$? To answer that question we can integrate (1.1) against a test function ϕ in V_h, then we obtain that

$$\int_\Omega \nabla \phi a \nabla u = \int_\Omega \phi g. \tag{1.36}$$

We will use the test function ϕ to "look at" the operator (1.1) at the given resolution h. We can decompose the first term in the integral above as a sum of integrals over the triangles of the coarse mesh to obtain (we assume that σ is stable)

$$\int_\Omega \nabla \phi a \nabla u = \sum_{K \in \mathcal{T}_h} \int_K \nabla \phi(x) a(x) \nabla F(x) \big(\nabla F(x)\big)^{-1} \nabla u(x)\, dx. \tag{1.37}$$

Now $\nabla\phi$ is constant within each triangle $K \in \mathcal{T}_h$. $\big(\nabla F(x)\big)^{-1}\nabla u(x)$ is Hölder continuous thus almost a constant within each triangle K and equal to the gradient of u evaluated on the coarse mesh with respect to the metric induced by F, i.e. the following vector

$$\nabla_F u(K) := \begin{pmatrix} F(b) - F(a) \\ F(c) - F(a) \end{pmatrix}^{-1} \begin{pmatrix} u(b) - u(a) \\ u(c) - u(a) \end{pmatrix}. \tag{1.38}$$

Where a, b, c are the nodes of the triangle K. It follows that the tensor $a\nabla F$ can be averaged over each triangle of the coarse mesh and we will write $< a\nabla F >_K$ its average. In conclusion a good candidate for the up-scaled operator $\mathcal{U}_h a$ is the bilinear form given by the following formula: for $v, w \in V_h$

$$\mathcal{U}_h a[v, w] := \sum_{K\in\mathcal{T}_h} \int_K {}^t\nabla v \big\langle a\nabla F \big\rangle_K \big(\nabla F(K)\big)^{-1}\nabla w. \tag{1.39}$$

Observe that the only information kept from the small scales in the compressed operator (1.39) are the bulk quantities $\big\langle a\nabla F\big\rangle_K$ and the non averaged quantities $F(b) - F(a)$ where a and b are nodes of the triangles of the coarse mesh. The latter quantity can be interpreted as a deformation of the coarse mesh induced by the small scales (or a new distance defining coarse gradients). In the particular case where $a = M(\frac{x}{\epsilon})$ and M is ergodic then as $\epsilon \downarrow 0 < a\nabla F >_K$ converges to the usual effective conductivity obtained from homogenization theory and $\nabla F(K)$ converges to the identity matrix. It follows that the object (1.39) recovers the formulae obtained from homogenization theory when the medium is ergodic and characterized by scale separation. Let us now show that formula (1.39) can be accurate beyond these assumptions.

To estimate the compression accuracy we have to use the up-scaled operator $\mathcal{U}_h a$ to obtain an approximation of the linear interpolation of u on the coarse mesh. We look for $u^m \in V_h$ such that for all $i \in \mathcal{N}_h$,

$$\mathcal{U}_h a[\varphi_i, u^m] = (\varphi_i, g)_{L^2(\Omega)}. \tag{1.40}$$

The price to pay for the loss of information on the small scales is the loss of ellipticity. This loss can be caused by two correlated factors:

- The new metric can generate flat triangles.
- The up-scaled operator can become singular.

The first factor is due to the localization of the scheme. The second factor does not appear with Galerkin schemes. It is not observed in dimension two but it can't be avoided in dimension higher or equal to three in the sense that the up-scaled operator has no reason to remain elliptic and local. Indeed consider a box of dimension three, and set in that box empty tubes

of low boundary conductivity as shown in figure 6. Set the left side of the box to temperature $0^0 c$ and the right side to temperature $100^0 c$. Then an inversion in the temperature profile is produced around the critical points shown in figure 6 (see [4] and [21], instead of increasing from left to right in these region temperature decreases). Now as the operator is up-scaled, the information on the geometry of the tubes is lost but the inversion phenomenon remains in the loss of ellipticity and locality of the operator. We will address this issue further in a forthcoming paper.

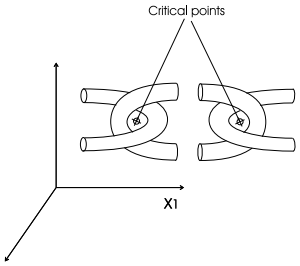

Figure 6: a in dimension three

Nevertheless it is possible to prove that once stability is achieved then the method is accurate (if σ is stable). More precisely, for a nodal function v let us define the homogeneous Dirichlet form on the graph induced by $\mathcal{T}_h$:

$$\mathcal{E}_h[v] := \sum_{i \sim j} |v_i - v_j|^2 \tag{1.41}$$

We write $i \sim j$ when those nodes share an edge on the coarse mesh. Let us define the following stability parameter of the scheme

$$\mathcal{S}^m := \inf_{w \in V_h} \sup_{v \in V_h} \frac{\mathcal{U}_h a[v,w]}{\big(\mathcal{E}_h[v]\big)^{\frac{1}{2}} \big(\mathcal{E}_h[w]\big)^{\frac{1}{2}}}. \tag{1.42}$$

Observe that $\mathcal{S}^m$ depends only on the up-scaled parameters so we have a control on the stability.

Definition 1.5. We say that the scheme is stable if and only if $\mathcal{S}^m > 0$.

Remark 1.22. Let us recall that for $v \in V_h$, $\mathcal{E}_h[v]$ can be bounded from below and above by the L^2-norm of the gradient of v. More precisely

$$\frac{1}{4\eta_{\max}} \mathcal{E}_h[v] \leq \|\nabla v\|^2_{L^2(\Omega)} \leq \eta_{\max} \mathcal{E}_h[v]. \tag{1.43}$$

$\eta_{\max} = 1/\sin(\theta)$ where θ is the closest interior angle of the triangles of $\mathcal{T}_h$ to 0 or π.

Remark 1.23. In practice in dimension two the condition number of the scheme associated to the up-scaled operator is as good as the one obtained from a Galerkin scheme by solving a local cell problem.

Let us write $\mathcal{I}_h u$ the linear interpolation of u over $\mathcal{T}_h$:

$$\mathcal{I}_h u := \sum_{i \in \mathcal{N}_h} u(x_i)\varphi_i(x). \tag{1.44}$$

We have the following estimate

Theorem 1.8. *Assume that σ and the scheme are stable and that the mesh is not unadapted to F. Then there exist constants $\alpha, C_m > 0$ such that*

$$\|\mathcal{I}_h u - u^m\|_{H^1(\Omega)} \leq C_m h^\alpha \|g\|_{L^\infty(\Omega)}. \tag{1.45}$$

Remark 1.24. The constant α depends only on n, Ω and μ_σ. The constant C_m can be written

$$C_m := C\frac{\eta^*_{\min}\eta_{\max}}{S^m}. \tag{1.46}$$

where C depends on the objects mentioned above plus $\lambda_{\min}(a), \lambda_{\max}(a)$ and $\left\| \left(\operatorname{Trace}(\sigma) \right)^{-1-\epsilon} \right\|_{L^1(\Omega)}$.

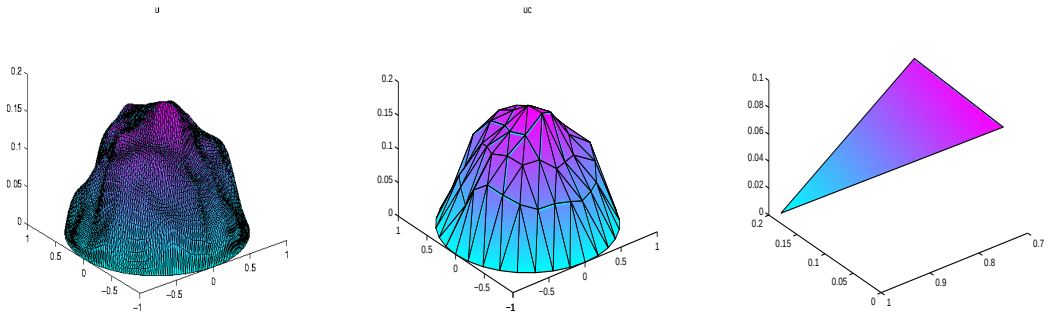

(a) u **(b)** u^m **(c)** ***Triangle of the coarse mesh.***

Figure 7: u estimated with the up-scaled operator.

The compressed operator allows us to capture the solution of (1.1) on a coarse mesh (figure 7). What information should be added to the compressed operator in order to obtain fine resolution approximation of u? The answer is a finer resolution of F (figure 8). Indeed let $\mathcal{J}_h$ be the interpolation operator introduced in (1.30), we then have the following estimate

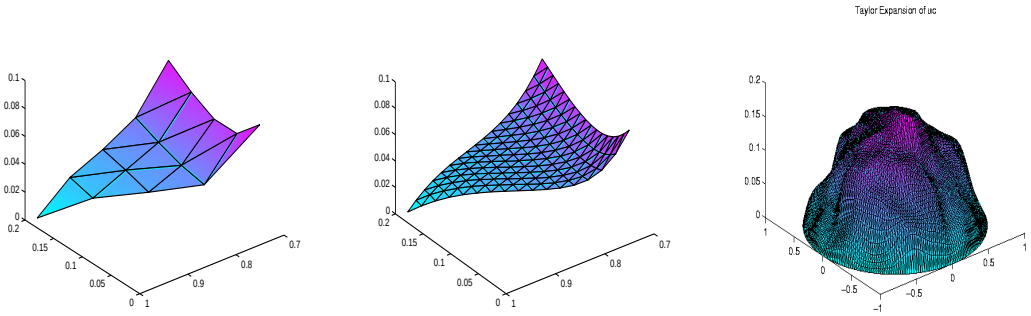

(a) ***Refined*** F**. .** **(b)** ***Refined*** F**.** **(c)** $\mathcal{J}_h u$**.**

Figure 8: Taylor expansion with respect to the new metric.

Theorem 1.9. *Assume that σ and the scheme are stable and that the mesh is not unadapted to F. Then there exist constants $\alpha, C_m > 0$ such that*

$$\|u - \mathcal{J}_h u^m\|_{H^1(\Omega)} \leq C_m h^\alpha \|g\|_{L^\infty(\Omega)}. \tag{1.47}$$

Remark 1.25. The constant α depends only on n, Ω and μ_σ. The constant C_m can be written

$$C_m := C\Big(\frac{\eta^*_{\max}\eta_{\max}}{S^m}\Big)^{\frac{1}{2}} \tag{1.48}$$

where C depends on the objects mentioned above plus $\lambda_{\min}(a), \lambda_{\max}(a)$ and $\big\|\big(\operatorname{Trace}(\sigma)\big)^{-1-\epsilon}\big\|_{L^1(\Omega)}$.

1.4.1 Coherent multi-resolution.

We want to compress a physical system from a fine scale description (F) to a coarse scale description (C) there are two ways of doing so:

- Either we up-scale directly from (F) to (C)
- Either we do so in two steps: from (F) to an intermediate scale (I), then from (I) to (C).

Now if the scales (F), (I) and (C) are not completely separated a technique solely based on averaging (up-scaling of bulk quantities) would produce two different results (depending on the presence of an intermediate step or not). Thus it is important to check the consistency of the numerical homogenization method if the metric information $F(x_i) - F(x_j)$ is up-scaled in addition to traditional bulk quantities $< a\nabla F >_K$.

Let $\mathcal{T}^0, \ldots, \mathcal{T}^n$ be a multi-resolution tessellation of Ω. Each $\mathcal{T}^i$ is a regular conformal tessellation of Ω. Moreover $\mathcal{T}^{i+1}$ is a refinement of $\mathcal{T}^i$.

Let us write V^i the space of piecewise linear functions on $\mathcal{T}^i$. We write $\mathcal{B}^i$ the space of bilinear operators on $\mathcal{T}^i$. We want to compress (up-scale) the bilinear operator $a[,]$ on the multi-grid $\mathcal{T}^0, \ldots, \mathcal{T}^n$. We assume that the smallest scale n is fine enough to capture the irregularities of a, in that case we define a^n such that for all $v, u \in V^n$

$$a^n[v,u] := a[v,u]. \tag{1.49}$$

Since the gradient of an element of V^n is constant within each triangle of $\mathcal{T}^n$, $a^n[,]$ can be defined by a mapping from $\mathcal{T}^n$ onto $\mathcal{M}_n$ the space of $n \times n$ constant matrices. We will write $a^n(K)$ the constant matrix associated[3] to $K \in \mathcal{T}^n$. Similarly each bilinear operator of $\mathcal{B}^i$ can be defined by mapping from $\mathcal{T}^i$ onto $\mathcal{M}_n$. We define for $k \leq p, \mathcal{U}^{k,p}$ the up-scaling operator mapping $\mathcal{B}^p$ onto $\mathcal{B}^k$ in the following way (we assume that the tessellations $\mathcal{T}_i$ are not unadapted to F and that the respective schemes are stable). Let $B \in \mathcal{B}^p$.

- Let $F \in V^p$ be the solution of

$$\begin{cases} B[v,F] = 0 \quad \text{for all} \quad v \in V^p \\ F = x \quad \text{on} \quad \Gamma^i. \end{cases} \tag{1.50}$$

  where we have written Γ^i the boundary of $\mathcal{T}^i$.

- The bilinear form $\mathcal{U}^{k,p}B$ is defined by its matrices $\mathcal{U}^{k,p}B(K)$ for $K \in \mathcal{T}^k$.

$$\mathcal{U}^{k,p}B(K) := \big\langle B\nabla F \big\rangle_K \big(\nabla F(K)\big)^{-1}. \tag{1.51}$$

  $\big\langle . \big\rangle_K$ stands for the averaging operator

$$\big\langle B\nabla F \big\rangle_K := \frac{1}{\mathrm{Vol}(K)} \sum_{T \in \mathcal{T}^p, T \subset K} \mathrm{Vol}(T) B(T) \nabla F(T). \tag{1.52}$$

For $k \leq p \leq q$, $\mathcal{U}$ satisfies the semi-group property

$$\mathcal{U}^{k,q} = \mathcal{U}^{k,p}\mathcal{U}^{p,q}. \tag{1.53}$$

Note also that $\mathcal{U}^{q,q} = I_d$. In particular if we define for $k \in \{1, \ldots, n\}$

$$a^k := \mathcal{U}^{k,n} a^n \tag{1.54}$$

as the up-scaled operator, the following semi-group property is satisfied: for $k \leq p \leq n$

$$a^k := \mathcal{U}^{k,p} a^p. \tag{1.55}$$

Semi-group properties (1.53), (1.55) are essential to the consistency and coherence of the numerical homogenization method.

[3] the bilinear form (1.49) can be written as a sum of integrals over $K \in \mathcal{T}^n$. ∇v and ∇u are constant over these triangles, thus a^n_K as a bilinear form over V^n is determined by a matrix.

1.5 Numerical homogenization from the transport point of view.

The elliptic operator appearing in (1.1) can be seen as the generator of a stochastic differential equation. This stochastic differential equation can reflect the transport process of a pollutant in a highly heterogeneous medium such as soil. The following operator $\Delta - \nabla V \nabla$ whose numerical homogenization is similar to the one of (1.1) can represent a physical system evolving in a highly irregular energy landscape V. The simple fact that this evolution taking place in a continuous domain can be captured by a Markov chain evolving on a graph is far from being obvious [72]. Our point of view here is to accurately simulate a Markov chain living on a fine graph by an "up-scaled" Markov chain living on a coarse graph. The main question is how to choose the the jump rate γ_{ij} of the random walk between the nodes of the coarse graph? The answer to that question is given by a finite volume method.

Let us write $\mathcal{T}_h^*$ the dual mesh associated to $\mathcal{T}_h$. $\mathcal{T}_h^*$ can be obtained by drawing segments from the midpoints of the edges of the triangles of $\mathcal{T}_h$ to an interior point in these triangles (the circumcenter to obtain a Voronoï tessellation but one can also choose the barycenter).

Let us write V_i the control volume associated to the node i of the primal mesh and χ_i the characteristic function of V_i. The finite volume method can be expressed in the following way: look for $u^v \in \mathcal{Z}_h$ ($\mathcal{Z}_h$ being the space spanned by the elements ξ_i introduced in (1.23)) such that for all $i \in \mathcal{N}_h$

$$a^*[\chi_i, u^v] = (\chi_i, g)_{L^2}. \tag{1.56}$$

Again, it follows from equation (1.56) that the only information kept from the scales are the usual bulk quantities (effective conductivities at the edges of the dual mesh) plus the metric information $F(b) - F(a)$ where a and b are nodes of the triangles of the primal mesh. Observe also that it is possible to generate with this finite volume method a coherent multi-resolution compression similar to the one introduced in subsection 1.4.1. According to (1.56) the good choice for the jump rates of the random walk should be

$$\gamma_{ij} = a^*[\chi_i, \xi_j] \quad \text{if} \quad i \sim j \quad \text{and} \quad i \neq j. \tag{1.57}$$

To properly describe the transport process one should look at a parabolic operator instead of the elliptic one. This issue will be addressed in [65], we will restrict ourselves to the elliptic case characterizing the equilibrium properties of the random walk. Let us write $\mathcal{S}^v$ the stability of the up-scaled finite volume operator. It is defined by

$$\mathcal{S}^v := \inf_{w \in \mathcal{Z}_h} \sup_{v \in \mathcal{Y}_h} \frac{a^*[v, w]}{(\mathcal{E}_h[v])^{\frac{1}{2}} (\mathcal{E}_h[w])^{\frac{1}{2}}}. \tag{1.58}$$

Theorem 1.10. *Assume that σ and the scheme are stable ($S^v > 0$) and that the mesh is not unadapted to F. Then there exist constants $\alpha, C_v > 0$ such that*

$$\|\mathcal{I}_h u - \mathcal{I}_h u^v\|_{H^1(\Omega)} \leq C_{v,1} h^\alpha \|g\|_{L^\infty(\Omega)} \tag{1.59}$$

and

$$\|u - \mathcal{J}_h u^v\|_{H^1(\Omega)} \leq C_{v,2} h^\alpha \|g\|_{L^\infty(\Omega)}. \tag{1.60}$$

Remark 1.26. The constant α depends only on n, Ω and μ_σ. The constant $C_{v,1}$ can be written

$$C_{v,1} := C \frac{\eta^*_{\min} \eta_{\max}}{S^m} \big(\lambda_{\max}(\sigma)\big)^{\frac{1}{2}}. \tag{1.61}$$

The constant $C_{v,2}$ can be written

$$C_{v,2} := C \Big(\frac{\lambda_{\max}(\sigma) \eta^*_{\max} \eta_{\max}}{S^v} \Big)^{\frac{1}{2}}. \tag{1.62}$$

C depends on the objects mentioned above plus $\lambda_{\min}(a), \lambda_{\max}(a)$ and $\big\| \big(\operatorname{Trace}(\sigma) \big)^{-1-\epsilon} \big\|_{L^1(\Omega)}$.

Remark 1.27. Observe that we need the additional condition $\lambda_{\max}(\sigma) < \infty$ to prove the convergence of the method. Numerical experiments show that although the finite volume method keeps very few information from small scales it is more stable and accurate than the method presented in 1.4 (it is also more stable and almost as accurate as Galerkin method in which the whole fine scale scale structure of F is up-scaled). That is why we believe that the constants (1.61) and (1.62) are not optimal.

1.6 Explicit formulae in laminar cases.

The harmonic coordinates can be explicitly computed in dimension one. In this subsection we will analyze a toy model to understand the effect of the new metric when the coefficients of the partial differential equations are characterized by an infinite number of overlapping scales. Our point is to show that new metric becomes multi-fractal.

Let $\Omega := (0,1)$. Let $V \in L^\infty(\Omega)$ and write $w(V)$ the weak solution of the following Dirichlet problem:

$$\begin{cases} -\frac{1}{2} e^{2V} \operatorname{div} \big(e^{-2V} \nabla w \big) = f \\ w = 0 \quad \text{on} \quad \partial\Omega. \end{cases} \tag{1.63}$$

With $f \in L^\infty(\Omega)$. We write $w(V)$ the solution of (1.63). Write μ_+ and μ_- the probability measures defined on the Borelian subset of $(0,1)$ by

$$\mu_+[0,x] := \frac{\int_0^x e^{2V(z)}dz}{\int_0^1 e^{2V(z)}dz} \quad \text{and} \quad \mu_-[0,x] := \frac{\int_0^x e^{-2V(z)}dz}{\int_0^1 e^{-2V(z)}dz}. \tag{1.64}$$

Define $D(V) := \left(\int_0^1 e^{2V(z)}dz \int_0^1 e^{-2V(z)}dz\right)^{-1}$. $D(V)$ is to put into correspondence with the bulk quantity $< a\nabla F >$ which is a constant in dimension one. Observe that (1.63) can be explicitly rewritten

$$-\frac{1}{2}\frac{d}{d\mu_-}D(V)\frac{d}{d\mu_+}u = f. \tag{1.65}$$

In that sense the metric based numerical homogenization is exact in dimension one. Equations such as (1.65) have been studied in dimension one in [39] and [38] in order to introduce a measure-theoretic way of defining differential operators on fractal sets on the real line.
Let V_n be a sequence in $L^\infty(\Omega)$. We call a probability measure non degenerate if and only if it is atom-less and the mass of any non void open subset of Ω is strictly positive. We have the following theorem

Theorem 1.11. *If $\mu_+^{V_n}$ and $\mu_-^{V_n}$ weakly converge to non degenerate probability measures μ_+ and μ_- then $D(V_n)w(V_n)$ converges pointwise to the unique solution of the following differential equation with Dirichlet boundary condition*

$$-\frac{1}{2}\frac{d}{d\mu_-}\frac{d}{d\mu_+}\psi = f. \tag{1.66}$$

In the case of classical homogenization observe that μ_+ and μ_- are simple Lebesgue probability measures on $[0,1]$.

Write $\mathbb{T}$ the torus of dimension one and side of length one and let $U \in C^1(\mathbb{T})$. Let $\rho \in \mathbb{N}/\{0,1\}$. Write T_ρ the scaling operator denied on the space of functions by $T_\rho U(x) := U(\rho x)$. Write

$$S_n U := \sum_{p=0}^{n-1} T_{\rho^p} U. \tag{1.67}$$

Take $V_n = S_n U$ in theorem 1.11. Then by Perron-Frobenius-Ruelle theorem [76], $\mu_+^{V_n}$ and $\mu_-^{V_n}$ weakly converge to some probability measure μ_+ and μ_- (eigenvectors of the Ruelle transfer operator) and it is easy to check that they are non degenerate. Let us notice that similarly it is possible to show that $-\frac{1}{n}\ln D(V_n)$ converges to the sum of topological pressures of U and $-U$ with respect to the shift induced by the multiplication by ρ on the space of ρ-adic decompositions [66], [14]. Theorem 1.11 is telling us that the

regularity of ψ corresponds to the regularity of $\mu_+[0,x]$ thus it is natural to wonder what is the regularity of that harmonic measure. To answer that question we will consider the paradigm of binomial measures. We refer to [68] for a detailed introduction to this subject, for the sake of completeness we will recall its main lines below in our framework. We take $U(x) \in L^\infty(\mathbb{T})$ with $(a \neq b)$

$$2U(x) = \begin{cases} a & \text{for} \quad 0 \leq x < \frac{1}{2} \\ b & \text{for} \quad \frac{1}{2} \leq x < 1. \end{cases} \tag{1.68}$$

Let us write

$$m_0 = \frac{e^a}{e^a + e^b} \quad \text{and} \quad m_1 = \frac{e^b}{e^a + e^b}. \tag{1.69}$$

Then $\mu_+^{V_n}$ weakly converges to μ_+ and that measure is self-similar in the sense that it satisfies

$$\mu_+([x,y]) = m_0 \mu_+([2x, 2y]) + m_1 \mu_+([2x-1, 2y-1]). \tag{1.70}$$

For $x \in (0,1)$ we write $x_1 x_2 \dots$ its 2-adic decomposition in the sense that $x = \sum_{n=0}^{\infty} x_n 2^n$. We write $I_{y_1,\dots,y_p}$ the cylinder of $x \in (0,1)$ such that $x_1 \dots x_p = y_1 \dots y_p$. μ_+ is atom-less but singular with respect to the Lebesgue measure. Moreover it is easy to check [68] that μ_+ and therefore ψ are Holder continuous and their Holder continuity exponent is not a constant. More precisely let us write

$$\alpha_n(x) := -\frac{\ln\left(\mu_+[I_{x_1 \dots x_n}]\right)}{n \ln 2} \tag{1.71}$$

and

$$\alpha(x) := \lim_{n \to \infty} \alpha_n(x). \tag{1.72}$$

Whenever this limit exists. This limit exists for almost all x (with respect to Lebesgue measure) and its value depends on the dyadic expansion of x. Writing $l_n(x)$ the number of one appearing in the first n digits of x we have

$$\alpha(x) = \lim_{n \to \infty} -(1 - \frac{l_n(x)}{\ln n}) \log_2(m_0) - \frac{l_n(x)}{\ln n} \log_2(m_1). \tag{1.73}$$

Thus $\alpha(x)$ can take all the values between $-\log_2(m_0)$ and $-\log_2(m_1)$. However for almost all x with respect to Lebesgue measure

$$\alpha(x) = -\frac{1}{2} \log_2(m_0 m_1) = -\frac{1}{\ln 2}\big(\frac{a+b}{2} - \ln(e^a + e^b)\big). \tag{1.74}$$

Now it is possible to obtain from large deviation theory ([31] theorem 2 and [68]) that

$$\mathbb{P}\Big(\alpha_n(x) \in (\alpha - \epsilon, \alpha + \epsilon)\Big) \to 1 + c^*(\alpha) \tag{1.75}$$

$\mathbb{P}$ being the uniform probability measure on $(0,1)$, $c(q) = 1 - \log_2(m_0^q + m_1^q)$ and c^* denotes the Legendre transform of c, i.e. $c^*(\alpha) = \inf_q \big(q\alpha - c(q)\big)$. Thus the metric associated to our up-scaling method is multi-fractal [40], [57], [51]. Let us recall that multi-fractal formalism was originally introduced to describe the regularity of the velocity field in Turbulence [40] and explaining intermittency.

1.7 Literature.

The issue of numerical homogenization partial differential equations with heterogeneous coefficients has received a great deal of attention and many methods have been proposed[4]. Let us mention a few of them.

- Multi-scale finite element methods [30], [64], [49], [46], [36], [42], [2].
- Multi-scale finite volume methods [54].
- Heterogeneous Multi-scale Methods [29].
- Wavelet based homogenization [41], [28], [23], [18], [7], [19].
- Residual free bubbles methods [20].
- Discontinuous enrichment methods [34], [33].
- Partition of Unity Methods [37].
- Energy Minimizing Multi-grid Methods [75].

The methods mentioned above are part of a larger quest aimed at capturing high dimensional problems with a few coarse parameters [69], [5], [62], [44] . Paraphrasing the outcome of a recent DOE workshop [27], we may understand the physics of multi-scale structures at each individual scale nevertheless *without the capability to bridge the scales, a significant number of important scientific and engineering problems will remain out of reach.*

2 Proofs.

2.1 Compensation.

Let us prove theorem 1.1. We need a variation of Campanato's result [22] on non-divergence form elliptic operators. Let us write for a symmetric matrix M,

$$\nu_M := \frac{\sum_{i=1}^n \lambda_{i,M}}{\sum_{i=1}^n \lambda_{i,M}^2}. \tag{2.1}$$

[4] Justified in dimension one, in the case of periodic or ergodic media with scale separation or in the case of partial differential equations with sufficiently smooth coefficients

We consider the following Dirichlet problem:

$$L_M v = f \tag{2.2}$$

with $L_M := \sum_{i,j=1}^n M_{ij}(x)\partial_i\partial_j$. We assume M to be elliptic and symmetric.

Theorem 2.1. *Assume that $\beta_M < 1$. If Ω is convex, then, there exists a real number $p > 2$ depending only on n, Ω and β_M such that if $f \in L^p(\Omega)$ the Dirichlet problem (2.2) has a unique solution satisfying*

$$\|v\|_{W_0^{2,p}(\Omega)} \leq \frac{C}{1-\beta_M^{\frac{1}{2}}}\|\nu_M f\|_{L^p(\Omega)}. \tag{2.3}$$

Remark 2.1. β_M is the Cordes parameter (1.8) associated to M.

Proof. Theorem 2.1 is a straightforward adaptation of theorem 1.2.1 of [56], for the sake of completeness we will give the main lines of ideas leading to estimate (2.3). Let us recall the Miranda-Talenti estimate [56].

Lemma 2.1. *Let $\Omega \subset \mathbb{R}^n$ be a bounded and convex domain of class C^2. Then for each $v \in W_0^{2,2}(\Omega)$ it results*

$$\int_\Omega \sum_{i,j=1}^n (\partial_i\partial_j v)^2\, dx \leq \int_\Omega (\Delta v)^2\, dx. \tag{2.4}$$

The Laplacian $\Delta : W_0^{2,p}(\Omega) \to L^p(\Omega)$ is an isomorphism for each $p > 1$. Let $\Delta^{-1}(p)$ be the inverse operator $\Delta^{-1} : L^p(\Omega) \to W_0^{2,p}$. It is clear from (2.4) that $\|\Delta^{-1}(2)\| \leq 1$. Let $r \in (2, \infty)$, by the convexity of the norms we have

$$\|\Delta^{-1}(p)\| \leq C(p) \tag{2.5}$$

with

$$C(p) := \|\Delta^{-1}(r)\|^{\frac{r(p-2)}{p(r-2)}}. \tag{2.6}$$

Let v be a solution of (2.2) (we refer to [56] for the existence of v which is obtained from a fix point theorem), we have

$$\|v\|_{W_0^{2,p}(\Omega)} \leq \|\Delta^{-1}(p)\|\|\Delta v\|_{L^p(\Omega)}. \tag{2.7}$$

Observing that $\Delta v = \nu_M f + \Delta v - \nu_M L_M v$ one can obtain

$$\|\Delta v\|_{L^p(\Omega)} \leq \|\nu_M f\|_{L^p(\Omega)} + \|\Delta v - \nu_M L_M v\|_{L^p(\Omega)}. \tag{2.8}$$

Then following the proof of theorem theorem 1.2.1 of [56] we have

$$\|\Delta v - \nu_M L_M v\|_{L^p(\Omega)}^p \leq \int_\Omega \beta_M^{p/2}\Big(\sum_{i,j=1}^n (\partial_i\partial_j v)^p\Big)\, dx. \tag{2.9}$$

Let us choose $p > 2$ such that $1 - C(p)\beta_M^{1/2} \geq (1 - \beta_M^{1/2})/2$. Combining (2.7), (2.8) and (2.9) we obtain that

$$\Big(\int_\Omega \big(\sum_{i,j=1}^n (\partial_i \partial_j v)^p \big)\, dx \Big)^{\frac{1}{p}} \leq \frac{2C(p)}{1 - \beta_M^{1/2}} \|\nu_M f\|_{L^p(\Omega)}. \tag{2.10}$$

Which leads to estimate (2.3). □

Remembering the Sobolev embedding inequality

$$\|\nabla v\|_{C^{1-\frac{n}{p}}(\bar{\Omega})} \leq C \|v\|_{W_0^{2,p}(\Omega)} \tag{2.11}$$

theorem 2.1 implies the Hölder continuity of v in dimension $n = 2$.

We assume that σ is stable. We write F^{-1} the inverse of F (which is well defined if σ is stable). Let us write Q the symmetric positive matrix given by the following equation

$$Q(y) := \Big(\frac{\big({}^t \nabla F a \nabla F\big)}{|\det\big(\nabla F\big)|} \Big) \circ F^{-1}(y). \tag{2.12}$$

Let us write w the solution of the following equation: for all $\hat{\varphi} \in C_0^\infty$,

$$\sum_{i,j=1}^n Q_{ij} \partial_i \partial_j w = -\frac{\hat{g}}{|\det\big(\nabla F\big)| \circ F^{-1}}. \tag{2.13}$$

Let us now prove the following theorem,

Theorem 2.2. *Assume that σ is stable and that Ω is convex. Then there exists constants $p > 2$, $C > 0$ such that the solution of (2.13) belongs to $W_0^{2,p}(\Omega)$ and satisfies*

$$\|\nabla w\|_{W_0^{2,p}(\Omega)} \leq \frac{C}{1 - \beta_\sigma^{\frac{1}{2}}} \|g\|_{L^\infty(\Omega)}. \tag{2.14}$$

Remark 2.2. α depends on Ω and β_σ. C depends on $\lambda_{\min}(a)$ and if $n \leq 4$ on $\big\| \big(\operatorname{Trace}(\sigma) \big)^{\frac{n}{2} - 2 - \epsilon} \big\|_{L^1(\Omega)}$.

Proof. Now let us observe that

$$\frac{\nu_Q}{\det(\nabla F) \circ F^{-1}} = \frac{\operatorname{Trace}(\sigma)}{\operatorname{Trace}(\sigma^2)} \circ F^{-1}. \tag{2.15}$$

Using the change of variables $y = F(x)$ and choosing $1/q' + 1/q = 1$ we obtain that

$$\Big\| \frac{\nu_Q}{\det(\nabla F) \circ F^{-1}} \hat{g} \Big\|_{L^p(\Omega)} \leq \|g\|_{L^{pq'}(\Omega)} \Big\| \frac{\operatorname{Trace}(\sigma)}{\operatorname{Trace}(\sigma^2)} (\det(\nabla F))^{\frac{1}{pq}} \Big\|_{L^{pq}(\Omega)}. \tag{2.16}$$

It is easy to check that

$$\Big\|\frac{\mathrm{Trace}(\sigma)}{\mathrm{Trace}(\sigma^2)}(\det(\nabla F))^{\frac{1}{pq}}\Big\|^{pq}_{L^{pq}(\Omega)} \leq \frac{C_{qp,n}}{(\lambda_{\min}(a))^{\frac{n}{2}}}\int_\Omega \big(\,\mathrm{Trace}(\sigma)\big)^{\frac{n}{2}-qp}. \quad (2.17)$$

For $2 \leq n \leq 4$ we choose $q = 1$ in (2.17) for $n \geq 5$ we choose $q = \frac{n}{2p}$. Then a direct application of theorem 2.1 and estimate (2.15) to equation (2.13) implies the theorem (observe that $\beta_Q = \beta_\sigma$). □

Let $\varphi \in C_0^\infty(\Omega)$. Write $\hat{\varphi} := \varphi \circ F^{-1}$. Using theorem 2.2 we obtain that

$$\Big(\hat{\varphi}, \sum_{i,j=1}^n Q_{ij}\partial_i\partial_j w\Big)_{L^2(\Omega)} = -\Big(\hat{\varphi}, \frac{\hat{g}}{|\det\big(\nabla F\big)| \circ F^{-1}}\Big)_{L^2(\Omega)}. \quad (2.18)$$

Using the change of variable $y = F(x)$ we deduce that

$$\Big(\varphi, \sum_{i,j=1}^n \sigma_{ij}(\partial_i\partial_j w) \circ F\Big)_{L^2(\Omega)} = -\Big(\varphi, g\Big)_{L^2(\Omega)}. \quad (2.19)$$

Let us observe that

$$\sum_{i,j=1}^n \sigma_{ij}(\partial_i\partial_j w) \circ F = \mathrm{div}\,\Big(a\nabla F\big((\nabla w) \circ F\big)\Big). \quad (2.20)$$

It follows after an integration by parts that (and observing that $\nabla F(\nabla w) \circ F = \nabla(w \circ F)$)

$$a[\varphi, w \circ F] = (\varphi, g)_{L^2(\Omega)} \quad (2.21)$$

It follows from the uniqueness of the solution of the Dirichlet problem (2.21) that $w \circ F = u$. Theorem 1.2 is then a straightforward consequence of theorem 2.2 and the equality $u \circ F^{-1} = w$.

Remark 2.3. Using the change of variables $y = F(x)$ we obtain for all $\varphi \in C_0^\infty(\Omega)$)

$$a[\varphi, u] = Q[\hat{\varphi}, \hat{u}] \quad (2.22)$$

The comparison between (2.18) and (2.22) indicates that Q is a divergence free matrix. We have not used that property of Q explicitly in our proof above but it is present implicitly in the deduction of (2.21) from (2.20).

Remark 2.4. The only place where we use the convexity of Ω is for the validity of lemma 2.1 (we refer to [56]).

The following lemma is a well known result obtained from the De Giorgi-Moser-Nash theory ([26], [59], [63]) of divergence form elliptic operators with discontinuous coefficients (more precisely we refer to [70] for the Global Hölder regularity)

Lemma 2.2. *There exists $C, \alpha' > 0$ depending on Ω and $\lambda_{\max}(a)/\lambda_{\min}(a)$ such that F is α' Hölder continuous and*

$$\|F\|_{C^{\alpha'}} \leq C. \tag{2.23}$$

Theorem 1.1 is a straightforward consequence of the Sobolev embedding inequality (2.11), theorem 2.2, lemma 2.1 and the fact that $\nabla_F u = \nabla \hat{u} \circ F$. Let us observe that in dimension two, we have

$$\frac{1}{1-\beta_\sigma} = \frac{1}{2}(\mu_\sigma + \frac{1}{\mu_\sigma}). \tag{2.24}$$

And the condition $\beta_\sigma < 1$ is equivalent to $\mu_\sigma < \infty$.

2.1.1 Hölder continuity for $n \geq 3$ or non-convexity of Ω.

In this subsection we will not assume Ω to be convex. Let $N^{p,\lambda}(\Omega)$ $(1 < p < \infty,\ 0 < \lambda < n)$ be the weighted Morrey space formed by functions $v : \Omega \to \mathbb{R}$ such that $\|v\|_{N^{p,\lambda}(\Omega)} < \infty$ with

$$\|v\|_{N^{p,\lambda}(\Omega)} = \sup_{x_0 \in \Omega} \Big(\int_\Omega |x - x_0|^{-\lambda} |v(x)|^p \Big)^{\frac{1}{p}}. \tag{2.25}$$

To obtain the Hölder continuity of $u \circ F^{-1}$ in dimension $n \geq 3$ we will use corollary 4.1 of [55]. We will give the result of S. Leonardi below in a form adapted to our context. Consider the Dirichlet problem (2.2). We do not assume Ω to be bounded. We write $W^{2,p,\lambda}(\Omega)$ the functions in $W^{2,p}(\Omega)$ such that their second order derivatives are in $N^{p,\lambda}(\omega)$.

Theorem 2.3. *There exist a constant $C^* = C^*(n, p, \lambda, \partial\Omega) > 0$ such that if $\beta_M < C^*$ and $f \in N^{p,\lambda}(\Omega)$ then the Dirichlet problem (2.2) has a unique solution in $W^{2,p,\lambda} \cap W_0^{1,p}(\Omega)$. Moreover, if $0 < \lambda < n < p$ then $\nabla v \in C^\alpha(\Omega)$ with $\alpha = 1 - n/p$ and*

$$\|\nabla v\|_{C^\alpha(\Omega)} \leq \frac{C}{\lambda_{\min}(M)} \|f\|_{N^{p,\lambda}(\Omega)} \tag{2.26}$$

where $C = C(n, p, \lambda, \partial\Omega)$.

Theorem 1.3 is a straightforward application of theorem 2.3.

2.2 Dimensionality reduction.

Let us prove theorem 1.4. We write X_h the linear space spanned by the elements ψ_i. The solution of the Galerkin scheme satisfies $a[u - u_h, v] = 0$ for all $v \in X_h$. Thus

$$a[u - u_h] = \inf_{v \in X_h} a[u - u_h, u - v]. \tag{2.27}$$

It follows by Cauchy-Schwartz inequality that

$$a[u-u_h] \leq \inf_{v\in X_h} a[u-v]. \tag{2.28}$$

Now writing $\hat{v} := v \circ F^{-1}$ and using the change of variable $y = F(x)$ we obtain

$$a[u-v] = Q[\hat{u}-\hat{v}]. \tag{2.29}$$

It follows in dimension $n = 2$ that

$$\|u-u_h\|^2_{H^1} \leq \frac{D}{\lambda_{\min}(a)} \inf_{w\in V_h} \|\nabla\hat{u} - \nabla w\|^2_{L^\infty(\Omega)} \tag{2.30}$$

with

$$D := \text{Trace}\Big[\int_\Omega {}^t\nabla F a \nabla F\Big]. \tag{2.31}$$

Thus using the following standard approximation properties of the elements φ_i (see for instance [32]),

$$\inf_{w\in V_h} \|\nabla\hat{u} - \nabla w\|_{L^2(\Omega)} \leq C\gamma(\mathcal{T}_h)h^\alpha \|\hat{u}\|_{C^{1,\alpha}_0(\Omega)} \tag{2.32}$$

we obtain that

$$\|u-u_h\|_{H^1} \leq \gamma(\mathcal{T}_h)\big(\frac{D}{\lambda_{\min}(a)}\big)^{\frac{1}{2}} \|\nabla\hat{u}\|_{C^\alpha} h^\alpha. \tag{2.33}$$

We conclude by observing that for $l \in \mathbb{R}^n$

$$\int_\Omega {}^t l^t\nabla F a \nabla F l = \inf_{f\in C^\infty_0(\Omega)} \int_\Omega {}^t(l+\nabla f) a (l+\nabla f). \tag{2.34}$$

Theorem 1.4 becomes a direct consequence of (2.30) and theorem 2.2.
In dimension $n \geq 3$ we obtain from (2.29) that

$$\|u-u_h\|^2_{H^1} \leq \frac{\lambda_{\max}(Q)}{\lambda_{\min}(a)} \inf_{w\in V_h} \|\nabla\hat{u} - \nabla w\|^2_{L^2(\Omega)}. \tag{2.35}$$

It is easy to obtain that

$$\lambda_{\max}(Q) \leq \big(\det(a)\big)^{\frac{1}{2}} \mu_\sigma^{\frac{n}{2}} \big(\text{Trace}(\sigma)\big)^{1-\frac{n}{2}}. \tag{2.36}$$

We conclude by observing that $\mu_\sigma < C(\beta_\sigma)$ and using the following standard approximation properties of the elements φ_i (see for instance [32]).

$$\inf_{w\in V_h} \|\nabla\hat{u} - \nabla w\|_{L^2(\Omega)} \leq C\gamma(\mathcal{T}_h)h \|\hat{u}\|_{W^{2,2}_0(\Omega)}. \tag{2.37}$$

2.3 Galerkin with localized elements.

Let us prove theorem 1.6. We assume that the coarse mesh is not unadapted to F. Let K be a triangle of $\mathcal{T}_h$ and let a be a node of K such that $\eta^F_{\min}(K) = \frac{1}{\sin\theta}$ where θ is the interior angle between $(F(a), F(b))$ and $(F(a), F(c))$; (b, c) being the other nodes of K. Let us prove the following lemma

Lemma 2.3.

$$|\nabla_F u(K) - \nabla_F u(a)| \leq 3\eta^F_{\min}(K)\|\nabla\hat{u}\|_{C^\alpha}\|F\|^\alpha_{C^{\alpha'}} h^{\alpha\alpha'}. \tag{2.38}$$

Proof. It is easy to check that

$$u(b) - u(a) = \big(F(b) - F(a)\big)\nabla\hat{u} \circ F(a) + (F(b) - F(a)) \cdot q_{ba}. \tag{2.39}$$

Where the vector q_{ba} is defined by

$$q_{ba} := \int_0^1 \Big[\nabla\hat{u}\big[F(a) + s(F(b) - F(a))\big] - \nabla\hat{u}\big[F(a)\big]\Big]\, ds. \tag{2.40}$$

We will use the notation $f_{ba} := (F(b) - F(a))/|F(b) - F(a)|$. We will write $f^\perp_{ba}$ the unit vector obtained by a 90^o rotation of f_{ba} towards f_{ca}. Defining q_{ca} as in (2.40) we obtain that

$$\nabla_F u(K) = \nabla_F u(a) + k \tag{2.41}$$

with

$$k = q_{ba} - \lambda f^\perp_{ba} \tag{2.42}$$

with

$$\lambda := \frac{f_{ca}.(q_{ba} - q_{ca})}{f_{ca}.f_{ba^\perp}}. \tag{2.43}$$

Which leads us to

$$|\nabla_F u(K) - \nabla_F u(a)| \leq \frac{3}{f_{ca}.f_{ba^\perp}}\|\nabla\hat{u}\|_{C^\alpha}\|F\|^\alpha_{C^{\alpha'}} h^{\alpha\alpha'}. \tag{2.44}$$

□

The following lemma is a direct consequence of lemma 2.3

Lemma 2.4. *Let $K \in \mathcal{T}_h$ and let $x \in \Omega$ then*

$$|\nabla_F u(K) - \nabla_F u(x)| \leq 3\eta^*_{\min}\|\nabla\hat{u}\|_{C^\alpha}(1 + \|F\|^\alpha_{C^{\alpha'}})\big(h + \mathrm{dist}(x, K)\big)^{\alpha\alpha'}. \tag{2.45}$$

Let us write $\mathcal{Z}_h u$ the interpolation of u over the space Z_h:

$$\mathcal{Z}_h u(x) = \sum_{i \in \mathcal{N}_h} u(x_i)\xi_i(x). \tag{2.46}$$

Lemma 2.5. *We have*

$$a^*[u - \mathcal{Z}_h u] \leq C\eta^*_{\min} \|\nabla \hat{u}\|_{C^\alpha} \|F\|^\alpha_{C^{\alpha'}} h^{\alpha\alpha'} D. \tag{2.47}$$

Proof. We have

$$a_K[u - \mathcal{Z}_h u] = \int_K {}^t\big(\nabla_F u(x) - \nabla_F u(K)\big)\sigma(x)\big(\nabla_F u(x) - \nabla_F u(K)\big)\, dx \tag{2.48}$$

with $\sigma(x) := {}^t\nabla F a \nabla F$. Using the change of variables $F(x) = y$ we obtain that

$$a_K[u - \mathcal{Z}_h u] = \int_{F(K)} {}^t\big(\nabla \hat{u}(y) - \nabla_F u(K)\big)Q(y)\big(\nabla \hat{u}(y) - \nabla_F u(K)\big)\, dy \tag{2.49}$$

from which we deduce that

$$a_K[u - \mathcal{Z}_h u] \leq \big(3\eta^*_{\min} \|\nabla \hat{u}\|_{C^\alpha} \|F\|^\alpha_{C^{\alpha'}} h^{\alpha\alpha'}\big)^2 \int_{F(K)} \sup_{|e|=1} {}^t e Q e. \tag{2.50}$$

Thus

$$a^*[u - \mathcal{Z}_h u] \leq C\big(\eta^*_{\min} \|\nabla \hat{u}\|_{C^\alpha} \|F\|^\alpha_{C^{\alpha'}} h^{\alpha\alpha'}\big)^2 D \tag{2.51}$$

where D has been defined by (2.31). □

Theorem 1.6 is implied by lemma 2.5, theorem 2.2, lemma 2.2 and the following inequality

$$a^*[u - u^f] \leq a^*[u - \mathcal{Z}_h u]. \tag{2.52}$$

Let us now prove theorem 1.7. By the triangle inequality

$$a\big[u - \mathcal{J}_h u^f\big] \leq a\big[u - \mathcal{J}_h u\big] + a\big[\mathcal{J}_h u - \mathcal{J}_h u^f\big]. \tag{2.53}$$

We write $\hat{\mathcal{J}}_h u := (\mathcal{J}_h u) \circ F^{-1}$. $\hat{\mathcal{J}}_h u$ is a linear interpolation of $\hat{u}$ on the tessellation $\mathcal{T}^F$. Now using the identity

$$a[u - \mathcal{J}_h u] = Q[\hat{u} - \hat{\mathcal{J}}_h u] \tag{2.54}$$

we obtain that

$$a[u - \mathcal{J}_h u] \leq \|\hat{u}\|_{C^\alpha} \hat{h}^\alpha D. \tag{2.55}$$

Where we have written $\hat{h}$ the maximal length of the edges of $\mathcal{T}^F$. Observe that $\hat{h} \leq h^{\alpha'} \|F\|_{C^{\alpha'}}$. Theorem 1.7 is a consequence of inequalities (2.53), (2.55), lemmas 2.6 and 2.5, theorem 2.2 and the following inequality

$$a^*\big[\mathcal{Z}_h u - u^f\big] \leq 2a^*\big[u - \mathcal{Z}_h u\big].$$

Lemma 2.6.

$$a\big[\mathcal{J}_h u - \mathcal{J}_h u^f\big] \leq 2^6 \eta^*_{\max} \mu_\sigma^{\frac{1}{2}} \eta^3_{\max} \big(\frac{\lambda_{\max}(a)}{\lambda_{\min}(a)}\big)^{\frac{1}{2}} a^*\big[\mathcal{Z}_h u - u^f\big] \tag{2.56}$$

and

$$a\big[\mathcal{J}_h u - \mathcal{J}_h u^f\big] \leq \mu_\sigma \nu^* a^*\big[\mathcal{Z}_h u - u^f\big] \tag{2.57}$$

Proof. Let us write $w := \mathcal{J}_h u - \mathcal{J}_h u^f$. We need to bound $a[w]$. We have

$$a[w] = \frac{a^*[\mathcal{J}_h w]}{a^*[\mathcal{Z}_h w]} a^*[\mathcal{Z}_h w]. \tag{2.58}$$

$a^*[\mathcal{Z}_h w] = a^*[\mathcal{Z}_h u - u^f]$ has already been estimated in lemma 2.5. Observe that

$$a^*[\mathcal{J}_h w] = Q[\hat{w}]. \tag{2.59}$$

$\hat{w}$ is piecewise linear on $\mathcal{T}^F$. Using property (1.43) we obtain that

$$Q[\hat{w}] \leq \eta^*_{\max} \lambda_{\max}(Q) \mathcal{E}_h[w]. \tag{2.60}$$

Moreover, observing that

$$Q \circ F = \frac{\sigma}{\big(\det(\sigma)\big)^{\frac{1}{2}}} \big(\det(a)\big)^{\frac{1}{2}} \tag{2.61}$$

we obtain that

$$\lambda_{\max}(Q) \leq \mu_\sigma^{\frac{1}{2}} \big(\det(a)\big)^{\frac{1}{2}}. \tag{2.62}$$

Equation (2.62) is valid in dimension 2, in dimension higher than 2 we would use the inequality (2.36)

$$\lambda_{\max}(Q) \leq \mu_\sigma^{\frac{1}{2}} \big(\lambda_{\min}(\sigma)\big)^{\frac{n-2}{2}} \big(\det(a)\big)^{\frac{1}{2}}. \tag{2.63}$$

We now need to bound from below $a^*[\mathcal{Z}_h w]/\mathcal{E}_h[w]$. For $K \in \mathcal{T}_h$ let us write $H(K)$ the matrix

$$H(K) := \int_K {}^t(\nabla F(K))^{-1} {}^t \nabla F(x) a \nabla F(x) (\nabla F(K))^{-1} \, dx. \tag{2.64}$$

We need to estimate $\inf_{|l|=1} {}^t l H(K) l$. Let us write a, b, c the nodes of K and

$$f(x) := \big(F(x) - F(a)\big)\big(\nabla F(K)\big)^{-1} \cdot l. \tag{2.65}$$

Let us observe that

$${}^t l H(K) l = \int_K {}^t \nabla f a \nabla f. \tag{2.66}$$

Moreover $f(a) = 0$, $f(b) = (b-a).l$ and $f(c) = (c-a).l$. Let us assume without loss of generality that $|f(b)|/|b-a| \geq |f(c)|/|c-a|$. Then

$$ {}^t l H(K) l \geq \inf_{w \in C^\infty(\Omega),\, w(a)=0,\, w(b)=f(b)} \int_K {}^t \nabla w a \nabla w. \tag{2.67} $$

The quantity appearing in (2.67) is the resistance metric distance between the points a and b and it is easy to check that (see for instance lemma 1.1 of [8])

$$ \inf_{w \in C^\infty(\Omega),\, w(a)=0,\, w(b)=f(b)} \int_K {}^t \nabla w a \nabla w \geq \lambda_{\min}(a)\, \mathrm{Vol}(K) \big(\frac{|f(b)|}{|b-a|} \big)^2. \tag{2.68} $$

Thus

$$ {}^t l H(K) l \geq \lambda_{\min}(a)\, \mathrm{Vol}(K) \big(\frac{|(b-a).l|}{|b-a|} \big)^2. \tag{2.69} $$

Let us observe that

$$ \frac{|(b-a).l|}{|b-a|} \geq \frac{1}{4\eta_{\max}}. \tag{2.70} $$

It follows that

$$ a^*[\mathcal{Z}_h w] \geq \|\nabla \mathcal{I}_h w\|^2_{L^2} \lambda_{\min}(a) \frac{1}{16 \eta^2_{\max}}. \tag{2.71} $$

Thus

$$ \frac{a^*[\mathcal{Z}_h w]}{\mathcal{E}_h[w]} \geq \lambda_{\min}(a) \frac{1}{2^6 \eta^3_{\max}}. \tag{2.72} $$

which leads us to equation (2.56).

Remark 2.5. One of the methods employed with non-conformal elements to ensure the stability and convergence of the scheme is the so called *patch test*. In our proof the stability condition and convergence is ensured by (2.72) and an uniform lower bound on $\eta_{\max}$.

To obtain (2.57) let us observe that

$$ a[w] = Q[\hat{w}]. \tag{2.73} $$

Thus

$$ a[w] = \sum_{K \in \mathcal{T}_h} \int_{K^F} {}^t \nabla \hat{w}(K^F) Q(y) \nabla \hat{w}(K^F)\, dy. \tag{2.74} $$

It follows that

$$ a[w] \leq \nu^* \sum_{K \in \mathcal{T}_h} \int_{F(K)} \frac{\lambda_{\max}(Q)}{\lambda_{\min}(Q)} {}^t \nabla \hat{w}(K^F) Q(y) \nabla \hat{w}(K^F)\, dy. \tag{2.75} $$

from equation (2.61) we obtain that

$$ \frac{\lambda_{\max}(Q)}{\lambda_{\min}(Q)} \leq \mu_\sigma. \tag{2.76} $$

Next, observing that

$$\sum_{K\in\mathcal{T}_h}\int_{F(K)} {}^t\nabla\hat{w}(K^F)Q(y)\nabla\hat{w}(K^F)\,dy = a^*[\mathcal{Z}_h w]. \tag{2.77}$$

we obtain (2.57). □

2.4 Numerical homogenization from the information point of view

In this subsection we will prove theorem 1.8 and theorem 1.9. The method introduced in subsection 1.4 can be formulated in the following way: look for $u^m \in V_h$ such that for all $i \in \mathcal{N}_h$,

$$a^*[\varphi_i, \mathcal{Z}_h u^m] = (\varphi_i, g)_{L^2\Omega} \tag{2.78}$$

which implies the following finite volume orthogonality property for all $i \in \mathcal{N}_h$,

$$a^*[\varphi_i, \mathcal{Z}_h u^m - u] = 0. \tag{2.79}$$

Let us write $w = u - \mathcal{Z}_h u^m$. By equation (1.42) we obtain that

$$\big(\mathcal{E}_h[w]\big)^{\frac{1}{2}} \leq \frac{1}{S^m}\sup_{v\in Z_h}\frac{a^*[v,\mathcal{Z}_h w]}{\big(\mathcal{E}_h[v]\big)^{\frac{1}{2}}}. \tag{2.80}$$

By the orthogonality property we have

$$a^*[v,\mathcal{Z}_h w] = a^*[v,\mathcal{Z}_h u - u]. \tag{2.81}$$

Thus

$$a^*[v,\mathcal{Z}_h w] \leq \big(\lambda_{\max}(a)\big)^{\frac{1}{2}}\|\nabla v\|_{L^2(\Omega)}\big(a^*[\mathcal{Z}_h u - u]\big)^{\frac{1}{2}}. \tag{2.82}$$

Using the inequality

$$\|\nabla v\|^2_{L^2(\Omega)} \leq \eta_{\max}\mathcal{E}_h[v]. \tag{2.83}$$

We deduce that

$$\mathcal{E}_h[w]^{\frac{1}{2}} \leq \frac{1}{S^m}\big(\lambda_{\max}(a)\eta_{\max}\big)^{\frac{1}{2}}\big(a^*[\mathcal{Z}_h u - u]\big)^{\frac{1}{2}}. \tag{2.84}$$

It follows from (1.43) that

$$\|\nabla\mathcal{I}_h u - \nabla u^m\|_{L^2(\Omega)} \leq \frac{\eta_{\max}}{S^m}\big(\lambda_{\max}(a)\big)^{\frac{1}{2}}\big(a^*[\mathcal{Z}_h u - u]\big)^{\frac{1}{2}}. \tag{2.85}$$

And we deduce from Poincaré inequality that

$$\|\mathcal{I}_h u - u^m\|_{L^2(\Omega)} \leq C_\Omega\frac{\eta_{\max}}{S^m}\big(\lambda_{\max}(a)\big)^{\frac{1}{2}}\big(a^*[\mathcal{Z}_h u - u]\big)^{\frac{1}{2}}. \tag{2.86}$$

We obtain theorem 1.8 by from equations (2.85), (2.86), lemma 2.5 and theorem 2.2. Let us now prove theorem 1.9. Using triangle inequality we obtain

$$a\big[u - \mathcal{J}_h u^m\big] \leq a\big[u - \mathcal{J}_h u\big] + a\big[\mathcal{J}_h u - \mathcal{J}_h u^m\big]. \tag{2.87}$$

The object $a\big[u - \mathcal{J}_h u\big]$ has already been bounded from above by (2.55). Writing $w := \mathcal{J}_h u - \mathcal{J}_h u^m$ we have

$$a[w] = \frac{a[\mathcal{J}_h w]}{\mathcal{E}_h[w]} \mathcal{E}_h[w]. \tag{2.88}$$

But $\mathcal{E}_h[w]$ has already been estimated in equation (2.84). It remains to notice that

$$a[\mathcal{J}_h w] = Q[\hat{w}]. \tag{2.89}$$

From this point the arguments are similar to the ones employed in subsection 2.3, indeed

$$Q[\hat{w}] \leq \lambda_{\max}(Q) \|\nabla \hat{w}\|_{L^2(\Omega)} \leq \eta^*_{\max} \lambda_{\max}(Q) \mathcal{E}_h[w]. \tag{2.90}$$

2.5 Numerical homogenization from a transport point of view.

We assume the mesh to be regular in the following sense: the nodes of the Vornoï diagram of $\mathcal{T}_h$ belong elements of the primal mesh. In dimension 2 this means that for each triangle $K \in \mathcal{T}_h$ the intersection of the median of K (the circumcenter) belongs to the interior of K. Let us write Y_h the vector space spanned by the functions χ_i. For $v \in Z_h$ we define $\mathcal{Y}_h v$ by

$$\mathcal{Y}_h v := \sum_{i \in \mathcal{N}_h} v_i \chi_i. \tag{2.91}$$

The metric numerical homogenization method can be formulated in the following way: look for $u^v \in Z_h$ (the space spanned by the elements ξ_i) such that for all $i \in \mathcal{N}_h$,

$$a^*[\chi_i, u^v] = (\chi_i, g)_{L^2\Omega} \tag{2.92}$$

which implies the following finite volume orthogonality property for all $i \in \mathcal{N}_h$,

$$a^*[\chi_i, u^v - u] = 0. \tag{2.93}$$

Equation (2.92) can be written

$$\sum_{j \sim i} u^v_j \int_{\partial V_i} n.a.\nabla \xi_i = \int_{V_i} g. \tag{2.94}$$

Let us write $w := \mathcal{Z}_h u - u^v$. From the equation (1.58) we obtain that

$$(\mathcal{E}_h[w])^{\frac{1}{2}} \leq \frac{1}{\mathcal{S}^v} \sup_{v \in \mathcal{Y}_h} \frac{a^*[v,w]}{(\mathcal{E}_h[v])^{\frac{1}{2}}}. \tag{2.95}$$

Using the orthogonality property of the finite volume method we obtain that for $v \in \mathcal{Y}_h$

$$a^*[v,w] = -\sum_{i \in \mathcal{N}_h} v_i \int_{\partial V_i} n.a\big(\nabla \mathcal{Z}_h u - \nabla u\big). \tag{2.96}$$

Writing $\mathcal{E}_h^*$ the edges of the dual tessellation (edges of the control volumes), we obtain that

$$a^*[v,w] = \sum_{e_{ij} \in \mathcal{E}_h^*} (v_j - v_i) \int_{e_{ij}} n_{ij}.a\big(\nabla \mathcal{Z}_h u - \nabla u\big). \tag{2.97}$$

Where e_{ij} is the edge separating the control volume V_i from the control volume V_j and n_{ij} is the unit vector orthogonal to e_{ij} pointing outside of V_i. It follows that

$$\begin{aligned} a^*[v,w] \leq & \big(\mathcal{E}_h[v]\big)^{\frac{1}{2}} \|\nabla_F \mathcal{Z}_h u - \nabla_F u\|_{L^\infty(\mathcal{E}_h^*)} \\ & \Big(\sum_{e_{ij} \in \mathcal{E}_h^*} |e_{ij}|^2 \lambda_{\max}(a) \lambda_{\max}(\sigma) \Big)^{\frac{1}{2}}. \end{aligned} \tag{2.98}$$

Now let us observe that

$$\sum_{e_{ij} \in \mathcal{E}_h^*} |e_{ij}|^2 \leq 3\eta_{\max} \operatorname{Vol}(\Omega). \tag{2.99}$$

We then have from equation (2.95)

$$\begin{aligned} \big(\mathcal{E}_h[w]\big)^{\frac{1}{2}} \leq & \frac{3}{\mathcal{S}^v} \|\nabla_F \mathcal{Z}_h u - \nabla_F u\|_{L^\infty(\mathcal{E}_h^*)} \\ & \eta_{\max} \operatorname{Vol}(\Omega) \big(\lambda_{\max}(a) \lambda_{\max}(\sigma)\big)^{\frac{1}{2}}. \end{aligned} \tag{2.100}$$

Equation (1.59) of theorem 1.10 is then a straightforward consequence of equation (1.43) and lemma 2.4. Let us now prove equation (1.60) of theorem 1.10. By triangle inequality

$$a\big[u - \mathcal{J}_h u^v\big] \leq a\big[u - \mathcal{J}_h u\big] + a\big[\mathcal{J}_h u - \mathcal{J}_h u^v\big]. \tag{2.101}$$

$a\big[u - \mathcal{J}_h u\big]$ has already been estimated in equation (2.55). Writing $w := \mathcal{J}_h u - \mathcal{J}_h u^v$ we have

$$a[w] = \frac{a^*[\mathcal{J}_h w]}{\mathcal{E}_h[w]} \mathcal{E}_h[w]. \tag{2.102}$$

But $\mathcal{E}_h[w]$ has already been estimated in equation 2.100. It remains to notice that $\frac{a^*[\mathcal{J}_h w]}{\mathcal{E}_h[w]}$ has already been estimated in equations (2.59) and (2.60) to conclude the proof.

3 Numerical Experiments

Let us now give illustrations of the implementation of this method. The domain is the unit disk in dimension two. Equation (1.1) is solved on a fine tessellation characterized by 66049 nodes and 131072 triangles. The coarse tessellation has 289 nodes and 512 triangles (figure 9). It is important to recall that since our methods involve the computation of global harmonic coordinates, the memory requirement and CPU time are not improved if one needs to solve (1.1) only one time, whereas localized methods such as the one of Hou and Wu or E. and Engquist do improve the memory requirement or the CPU time.

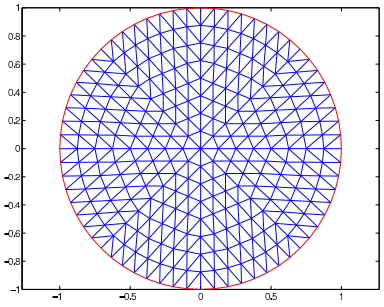

Figure 9: Coarse Grid

The elliptic operator associated to equation (1.1) has been up-scaled to an operator defined on the coarse mesh (compression by a factor of 300) using 5 different methods:

- The Galerkin scheme described in subsection 1.2 using the multiscale finite element ψ_i noted FEM_ψ.
- The Galerkin scheme described in subsection 1.3 using the localized elements ξ_i noted FEM_ξ.
- The metric based compression scheme described in subsection 1.4 noted MBFEM.
- The finite volume method described in subsection 1.5 noted FVM.
- A multi-scale finite element method noted LFEM where F is computed locally[5] on each triangle K of the coarse mesh as the solution of a cell problem with boundary condition $F(x) = x$ on ∂K. This method has been implemented in order to understand the effect of the removal of global information in the structure of the metric induced by F.

[5]instead of globally

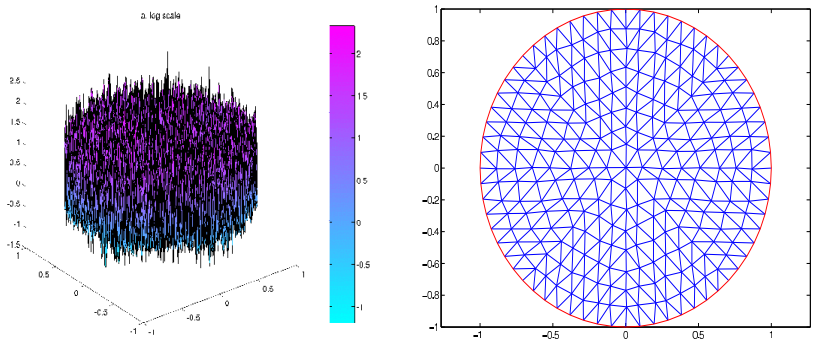

(a) a. **(b)** $\mathcal{T}^F$

Figure 10: Example 1, Trigonometric multi-scale.

Example 1. Trigonometric multiscale

$a(x) = \frac{1}{6}(\frac{1.1+\sin(2\pi x/\epsilon_1)}{1.1+\sin(2\pi y/\epsilon_1)} + \frac{1.1+\sin(2\pi y/\epsilon_2)}{1.1+\cos(2\pi x/\epsilon_2)} + \frac{1.1+\cos(2\pi x/\epsilon_3)}{1.1+\sin(2\pi y/\epsilon_3)} + \frac{1.1+\sin(2\pi y/\epsilon_4)}{1.1+\cos(2\pi x/\epsilon_4)} + \frac{1.1+\cos(2\pi x/\epsilon_5)}{1.1+\sin(2\pi y/\epsilon_5)} + \sin(4x^2y^2) + 1)$, where $\epsilon_1 = \frac{1}{5}$,$\epsilon_2 = \frac{1}{13}$,$\epsilon_3 = \frac{1}{17}$,$\epsilon_4 = \frac{1}{31}$,$\epsilon_5 = \frac{1}{65}$.

Figure 10 is an illustration of $\mathcal{T}^F$ the deformation of the coarse mesh (figure 9) under the metric induced by F. The deformation is small since the medium is quasi-periodic. The weak aspect ratio for triangles the coarse mesh in the metric induced by F is $\eta^*_{\text{min}} = 1.1252$. Table 1 gives the relative error estimated on the nodes of the coarse mesh between the solution u of the initial PDE (1.1) and an approximation obtained from the up-scaled operator on the nodes of the coarse mesh. Table 2 gives the relative error estimated on the nodes of the fine mesh between u and the $\mathcal{J}_h$-interpolation of the previous approximations with respect to F on a fine resolution. Figure 11(a) gives the condition number of the stiffness matrix associated to the up-scaled operator versus $-\log_2 h$ (logarithm of the resolution). Figure 11(b) gives the relative L_1-distance between u and its approximation on the coarse mesh in log scale versus $-\log_2 h$ (logarithm of the resolution). Observe that for the method LFEM this error increase with the resolution this is an effect of the so called cell resonance observed in [50] and [2]. This cell resonance does not occur with the methods proposed in this paper. The finite volume method is characterized by the the best stability and one of the best accuracy at a coarse resolution. The increase in the error observed for this method as the resolution is decreased is a numerical artifact created by the fine mesh: one has to divide the coarse tessellation into coarse control volumes. These coarse control volumes are unions of the control volumes defined on a fine mesh and when the refinement between the coarse and

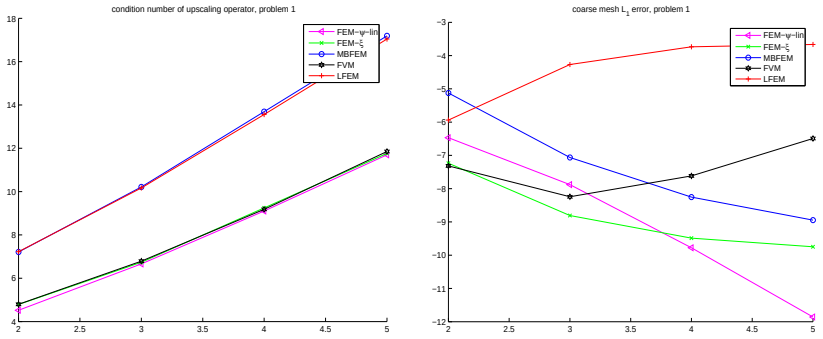

(a) *Condition Number.* **(b) *Coarse Mesh* L^1 *error.***

Figure 11: Example 1, Trigonometric Multiscale

Coarse Mesh Error	FEM_ψ	FEM_ξ	MBFEM	FVM	LFEM
L^1	0.0042	0.0022	0.0075	0.0032	0.0411
L^2	0.0039	0.0024	0.0074	0.0040	0.0441
L^∞	0.0059	0.0090	0.0154	0.0117	0.0496
H^1	0.0060	0.0262	0.0568	0.0203	0.0763

Table 1: Example 1, Trigonometric multi-scale.

Fine mesh Error	FEM_ψ	FEM_ξ	MBFEM	FVM	LFEM
L^1	0.0042	0.0085	0.0053	0.0080	0.0593
L^2	0.0043	0.0082	0.0061	0.0078	0.0591
L^∞	0.0063	0.0112	0.0154	0.0141	0.0597
H^1	0.0581	0.0540	0.0778	0.0601	0.0943

Table 2: Example 1, Trigononmetric Multiscale

the fine mesh is small and the triangulation irregular it is not possible to divide the coarse tessellation into control volumes intersecting the edges of the primal mesh close to the midpoints of those edges and the other control volumes close to the barycenters of the coarse triangles.

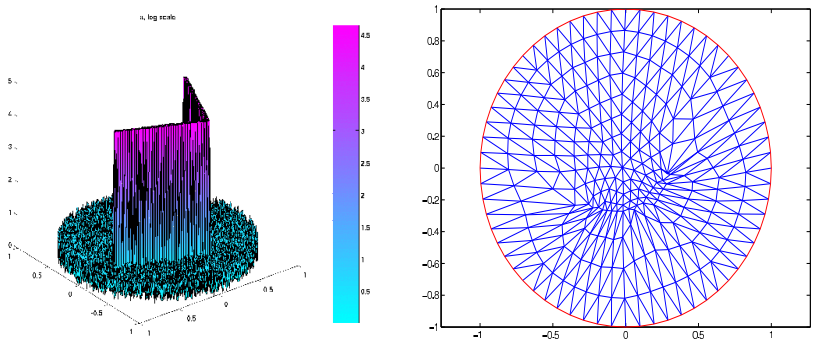

(a) a**.** **(b)** $\mathcal{T}^F$

Figure 12: Example 2, High Conductivity Channel.

Example 2. High Conductivity channel

In this example a is random and characterized by a fine and long ranged high conductivity channel. We choose $a(x) = 100$, if x is in the channel, and $a(x) = O(1)$, if x is not in the channel. The weak aspect ratio for triangles the coarse mesh in the metric induced by F is $\eta^{\star}_{\text{min}} = 2.2630$. Table 3 gives the relative error estimated on the nodes of the coarse mesh between the solution u of the initial PDE (1.1) and an approximation obtained from the up-scaled operator on the nodes of the coarse mesh. Table 4 gives the relative error estimated on the nodes of the fine mesh between u and the $\mathcal{J}_h$-interpolation of the previous approximations with respect to F on a fine resolution. Figure 13(a) gives the condition number of the stiffness matrix associated to the up-scaled operator versus $-\log_2 h$ (logarithm of the resolution). Figure 13(b) gives the relative L_1-distance between u and its approximation on the coarse mesh in log scale versus $-\log_2 h$.

Observe in figure 12 that the effect of the new metric on the mesh is to bring close together nodes linked by a path of low electrical resistance.

Remark 3.1. Let us recall that the natural distance associated to the Laplace operator on a fractal space is also the so called resistance metric [53], [71], [8]. It is thus natural to find that a similar (not equivalent) notion of distance allows the numerical homogenization PDEs with arbitrary coefficients. More precisely the analogue of the resistance metric here are the harmonic mappings. The analysis of these mappings allows to bypass boundary layers effects in homogenization in periodic media [2], it allows to obtain quantitative estimates on the heat kernel of periodic operators [66] or to analyze PDEs characterized by an infinite number of non separated scales [14], [67].

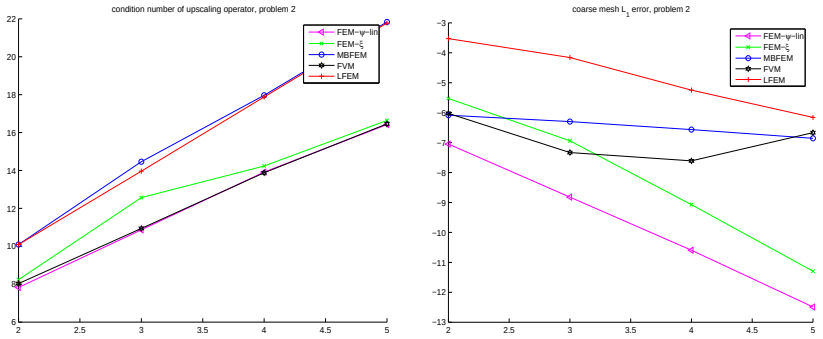

(a) *Condition Number.* **(b) *Coarse Mesh* L^1 *error.***

Figure 13: Example 2, High Conductivity Channel

Coarse Mesh Error	FEM_ψ	FEM_ξ	MBFEM	FVM	LFEM
L^1	0.0022	0.0081	0.0127	0.0062	0.0519
L^2	0.0025	0.0096	0.0179	0.0081	0.0606
L^∞	0.0120	0.0227	0.0549	0.0174	0.1223
H^1	0.0120	0.0384	0.0919	0.0265	0.1514

Table 3: Example 2, High Conductivity Channel.

Fine mesh Error	FEM_ψ	FEM_ξ	MBFEM	FVM	LFEM
L^1	0.0070	0.0155	0.0164	0.0121	0.0612
L^2	0.0069	0.0153	0.0202	0.0123	0.0743
L^∞	0.0133	0.0227	0.0573	0.0214	0.1226
H^1	0.0760	0.1032	0.1838	0.0820	0.2142

Table 4: Example 2, High Conductivity Channel.

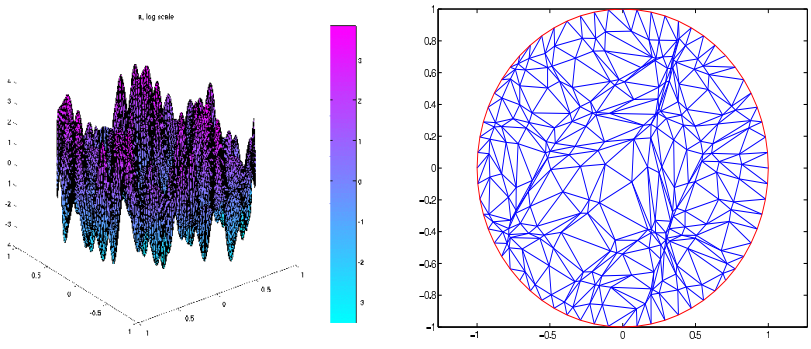

(a) a. **(b)** $\mathcal{T}^F$

Figure 14: Example 3, Random Fourier Modes .

Example 3. Random Fourier modes.

In this case, $a(x) = e^{h(x)}$, with

$$h(x) = \sum_{|k| \leq R} (a_k \sin(2\pi k \cdot x) + b_k \cos(2\pi k \cdot x))$$

where a_k and b_k are independent identically distributed random variables on $[-0.3, 0.3]$ and $R = 6$. This is an other example where scales are not separated. The weak aspect ratio of the triangles in the metric induced by F is $\eta^{\star}_{\min} = 3.4997$. Observe the deformation induced by the new metric (figure 14). Observe that distances between u and the interpolation of the coarse mesh approximations to the fine mesh are larger (tables 5 and 6), this is due to the fact that those errors depend on the aspect ratio $\eta^{*}_{\max}$ (which is not the case for the coarse mesh errors) of course one could improve the compression by adapting the mesh to the new metric but this has not been our point of view here. We have preferred to show raw data obtained with a given coarse mesh. The figures 16 and 17 give the L^1, L^2, L^∞ and H^1 relative error ($\log_2$ basis versus $\log_2$ basis of the resolution). The x-axis corresponds to the refinement of coarse mesh, the y-axis is the error. The tables 7 and 8 give the convergence rate in different norms (the parameter α in the error of the order of h^α).

Coarse Mesh Error	FEM_ψ	FEM_ξ	MBFEM	FVM	LFEM
L^1	0.0027	0.0075	0.0117	0.0106	0.1197
L^2	0.0028	0.0087	0.0130	0.0125	0.1169
L^∞	0.0066	0.0278	0.0320	0.0376	0.1358
H^1	0.0133	0.0648	0.0805	0.0597	0.1514

Table 5: Example 3, Random Fourier Modes

Fine mesh Error	FEM_ψ	FEM_ξ	MBFEM	FVM	LFEM
L^1	0.0112	0.0148	0.0148	0.0188	0.1304
L^2	0.0177	0.0223	0.0184	0.0202	0.1265
L^∞	0.0773	0.0824	0.0614	0.0680	0.1669
H^1	0.0972	0.1152	0.1307	0.1659	0.1725

Table 6: Example 3, Random Fourier Modes.

Method	L^1	L^2	L^∞	H^1
FEM_ψ	1.62	1.66	1.56	1.44
FEM_ξ	1.38	1.27	1.23	1.18
MBFEM	1.38	1.40	1.27	1.08
FVM	0.53	1.14	1.26	1.03
LFEM	1.51	1.53	1.62	1.46

Table 7: Coarse mesh approximation convergence rate

Method	L^1	L^2	L^∞	H^1
FEM_ψ	1.74	1.61	1.23	0.89
FEM_ξ	1.57	1.47	1.23	0.91
MBFEM	1.54	1.52	1.21	0.96
FVM	0.75	1.16	1.22	0.58
LFEM	1.52	1.54	1.42	1.10

Table 8: Fine mesh approximation convergence rate

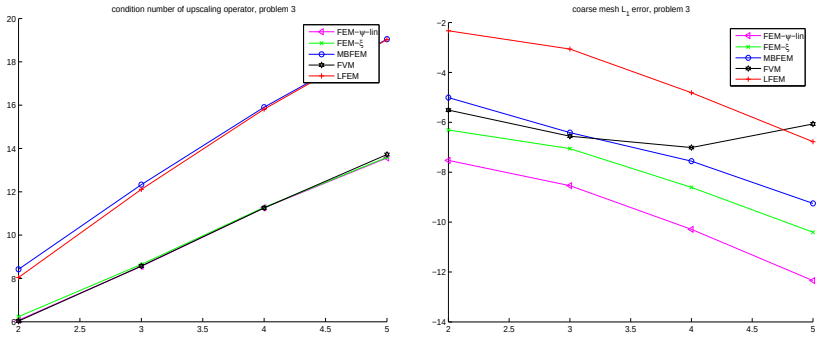

(a) *Condition Number.* **(b) *Coarse Mesh* L^1 *error.***

Figure 15: Example 3, Random Fourier Modes

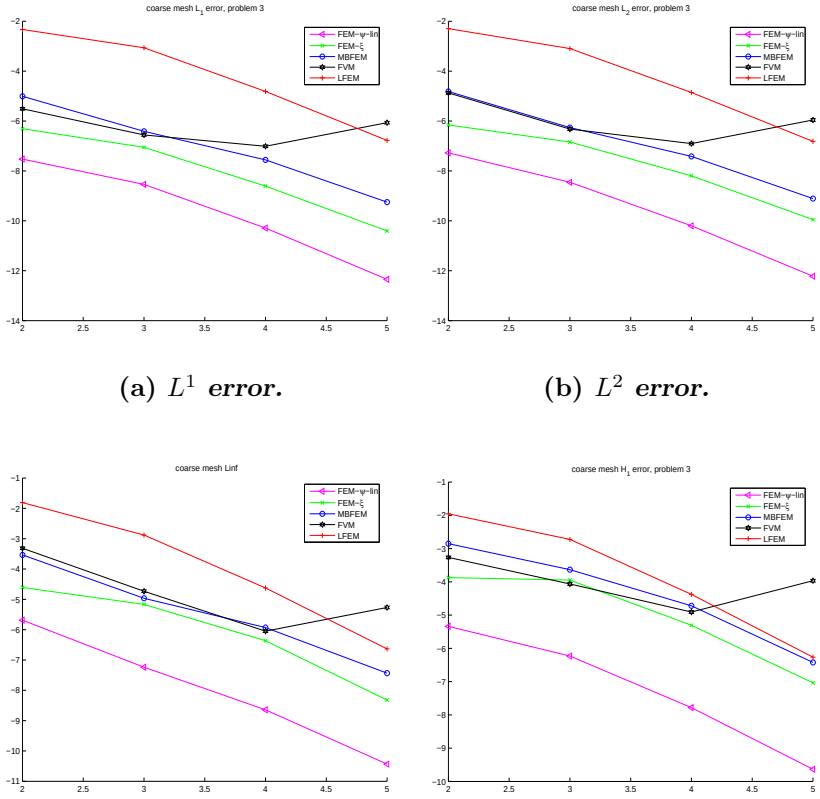

(a) L^1 ***error.*** **(b)** L^2 ***error.***

(c) L^∞ ***error.*** **(d)** H^1 ***error.***

Figure 16: Coarse mesh error ($\log_2$) L^1, L^2, L^∞ and H^1 errors v.s coarse mesh refinement, Example 3, Random Fourier Modes.

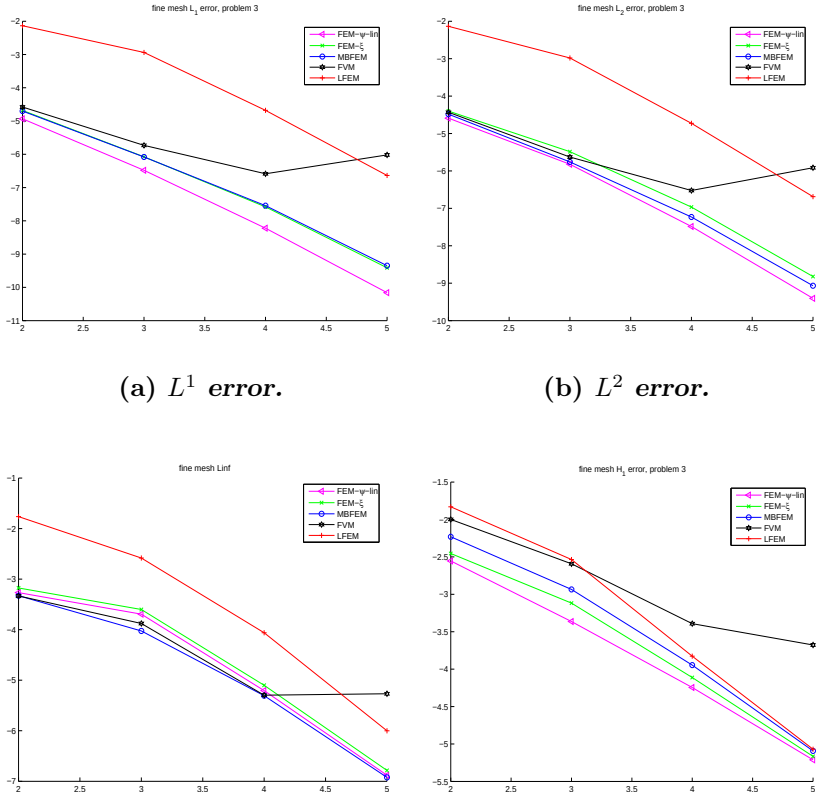

(a) L^1 ***error.*** **(b)** L^2 ***error.***

(c) L^∞ ***error.*** **(d)** H^1 ***error.***

Figure 17: Fine mesh approximation error ($\log_2$) L^1, L^2, L^∞ and H^1 errors v.s coarse mesh refinement, Example 3, Random Fourier Modes.

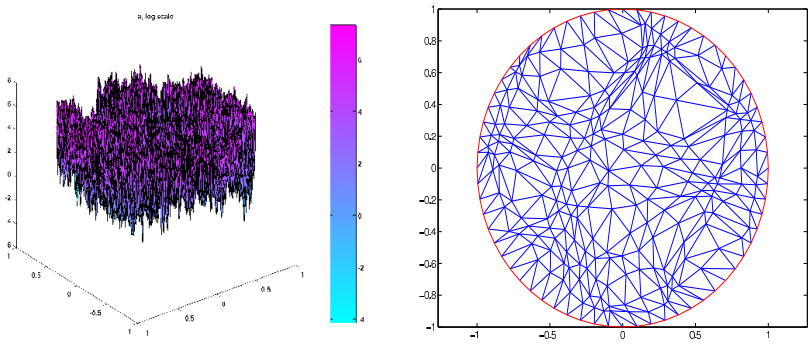

(a) a. **(b)** $\mathcal{T}^F$

Figure 18: Example 4, Random Fractal.

Coarse Mesh Error	FEM_ψ	FEM_ξ	MBFEM	FVM	LFEM
L^1	0.0024	0.0075	0.0231	0.0073	0.0519
L^2	0.0025	0.0085	0.0241	0.0100	0.0606
L^∞	0.0094	0.0399	0.0920	0.0398	0.1694
H^1	0.0161	0.0718	0.1553	0.0493	0.3107

Table 9: Example 4, Random Fractal.

Example 4. Random fractal

In this case, a is given by a product of discontinuous functions oscillating randomly at different scales, $a(x) = a_1(x)a_2(x)\cdots a_n(x)$, and $a_i(x) = c_{pq}$ for $x \in [\frac{p}{2^i}, \frac{p+1}{2^i}) \times [\frac{q}{2^i}, \frac{q+1}{2^i})$, c_{pq} is uniformly random in $[\frac{1}{\gamma}, \gamma]$, $n = 5$, and $\gamma = 2$. The weak aspect ratio is $\eta^\star_{\min} = 2.4796$. Table 9 gives the relative error estimated on the nodes of the coarse mesh between the solution u of the initial PDE (1.1) and an approximation obtained from the up-scaled operator on the nodes of the coarse mesh. Table 10 gives the relative error estimated on the nodes of the fine mesh between u and the $\mathcal{J}_h$-interpolation of the previous approximations with respect to F on a fine resolution. Figure 19(a) gives the condition number of the stiffness matrix associated to the up-scaled operator versus $-\log_2 h$ (logarithm of the resolution). Figure 19(b) gives the relative L_1-distance between u and its approximation on the coarse mesh in log scale versus $-\log_2 h$.

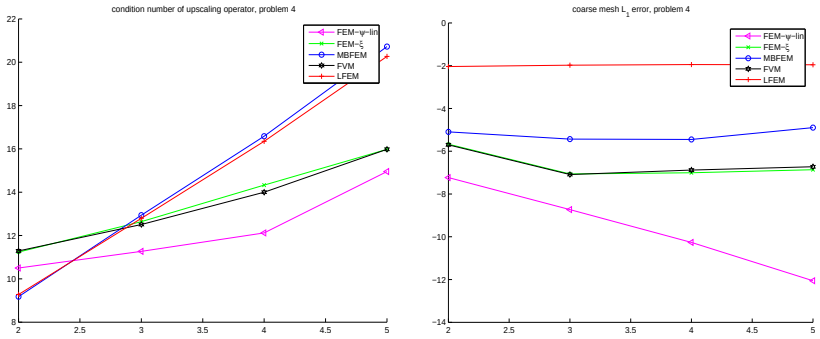

(a) *Condition Number.* **(b) *Coarse Mesh* L^1 *error.***

Figure 19: Example 4, Random Fractal

Fine mesh Error	FEM_ψ	FEM_ξ	MBFEM	FVM	LFEM
L^1	0.0108	0.0147	0.0245	0.0142	0.0765
L^2	0.0155	0.0198	0.0280	0.0173	0.0812
L^∞	0.0662	0.0802	0.0919	0.0720	0.1694
H^1	0.1015	0.1231	0.1838	0.1433	0.2642

Table 10: Example 4, Random Fractal.

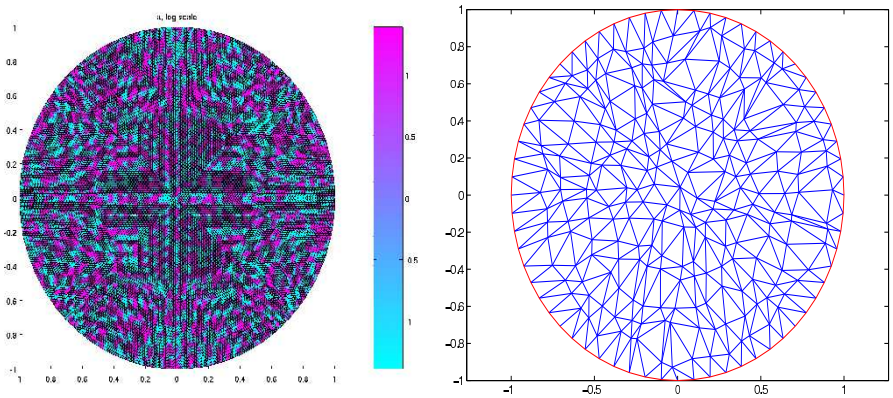

(a) a**.** **(b)** $\mathcal{T}^F$**.**

Figure 20: Example 5, Percolation.

Example 5. Percolation at criticality

In this case, the conductivity of each site is equal to γ or $1/\gamma$ with probability $1/2$. We have chosen $\gamma = 4$ in this example. Observe that some errors are larger for this challenging case because a percolating medium generates flat triangles in the new metric, indeed $\eta^{\star}_{\text{min}} = 22.3395$. Table 11 gives the relative error estimated on the nodes of the coarse mesh between the solution u of the initial PDE (1.1) and an approximation obtained from the up-scaled operator on the nodes of the coarse mesh. Table 12 gives the relative error estimated on the nodes of the fine mesh between u and the $\mathcal{J}_h$-interpolation of the previous approximations with respect to F on a fine resolution. Figure 21(a) gives the condition number of the stiffness matrix associated to the up-scaled operator versus $-\log_2 h$ (logarithm of the resolution). Figure 21(b) gives the relative L_1-distance between u and its approximation on the coarse mesh in log scale versus $-\log_2 h$. Observe that the methods based on a global change of metric do converge but when that numerical homogenization is done by computing only local coarse parameters (in averaging or finite elements techniques) then convergence is not guaranteed without further assumptions on a (see the curve of LFEM).

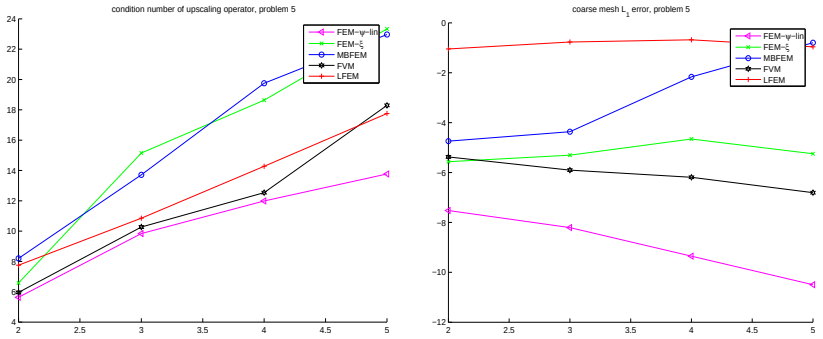

(a) *Condition Number.* **(b) *Coarse Mesh* L^1 *error.***

Figure 21: Example 5, Percolation

Coarse Mesh Error	FEM_ψ	FEM_ξ	MBFEM	FVM	LFEM
L^1	0.0034	0.0253	0.0485	0.0167	0.2848
L^2	0.0041	0.0265	0.0523	0.0189	0.2851
L^∞	0.0163	0.0813	0.0643	0.0499	0.3018
H^1	0.0343	0.0843	0.1070	0.0713	0.3740

Table 11: Example 5, Percolation.

Fine mesh Error	FEM_ψ	FEM_ξ	MBFEM	FVM	LFEM
L^1	0.0115	0.0265	0.0585	0.0216	0.3024
L^2	0.0152	0.0268	0.0628	0.0229	0.3015
L^∞	0.0500	0.0527	0.0940	0.0497	0.3135
H^1	0.1000	0.1712	0.1954	0.1343	0.3964

Table 12: Example 5, Percolation.

Coarse Mesh Error	FEM_ψ_{lin}	FEM_ψ_{sp}
L^1	0.0437	0.0046
L^2	0.0426	0.0052
L^∞	0.0614	0.0096
H^1	0.0746	0.0227

Table 13: Example 3, Random Fourier Modes

3.1 Numerical experiments with splines.

We have seen that if σ is stable then $u \circ F^{-1}$ belongs to $W^{2,p}(\Omega)$ with $p > 2$. It is thus natural to expect a better accuracy by using C^1-continuous elements in the method described in subsection 1.2 instead of piecewise linear elements. This increase of accuracy has already been observed in [2] when F is obtained as the solution of a local cell problem. In our case (the harmonic coordinates are computed globally) we also observe a sharp increase of the accuracy of finite element method of subsection 1.2 by using splines for the elements φ_i.

We refer to [48, 24] for methods using C^1 finite element. One possibility is the weighted extened B-splines (WEB) method developed by K. Höllig in [47, 48], these elements are C^2-continuous. They are obtained from tensor products of one dimensional elements. The Dirichlet boundary condition is satisfied using a smooth weight function ω, such that $\omega = 0$ at the boundary. The condition number of the stiffness matrix is bounded from above by $O(h^{-2})$ (we have the same optimal bound on a Galerkin system with piecewise linear elements).

We have considered two challenging multi-scale medium for our numerical experiments: random Fourier modes and percolation. For the simplicity of the implementation a square domain has been considered, and weighted spline basis are used instead of the WEB spline basis. For a square domain $[-1, 1] \times [-1, 1]$, the weight is $\omega = (1 - x^2)(1 - y^2)$. Two methods have been compared,

- The Galerkin scheme using the finite elements $\psi_i = \varphi_i \circ F$, where φ_i are the piecewise linear nodal basis elements of subsection 1.2, noted FEM_ψ_{lin}
- The Galerkin scheme using the finite element $\psi_i = \phi_i \circ F$, where ϕ_i are weighted cubic B-spline basis elements, noted FEM_ψ_{sp}

The error obtain with the method FEM_ψ_{sp} is much smaller than the one obtained with the method FEM_ψ_{lin} as it is shown in figures 22 and 23.

Fine mesh Error	FEM_ψ_{lin}	FEM_ψ_{sp}
L^1	0.0546	0.0077
L^2	0.0529	0.0096
L^∞	0.0920	0.0289
H^1	0.2109	0.0547

Table 14: Example 3, Random Fourier Modes.

Coarse Mesh Error	FEM_ψ_{lin}	FEM_ψ_{sp}
L^1	0.0393	0.0080
L^2	0.0379	0.0098
L^∞	0.0622	0.0309
H^1	0.0731	0.0404

Table 15: Example 5, Percolation

Fine mesh Error	FEM_ψ_{lin}	FEM_ψ_{sp}
L^1	0.0470	0.0099
L^2	0.0464	0.0130
L^∞	0.1174	0.0554
H^1	0.2030	0.0838

Table 16: Example 5, Percolation.

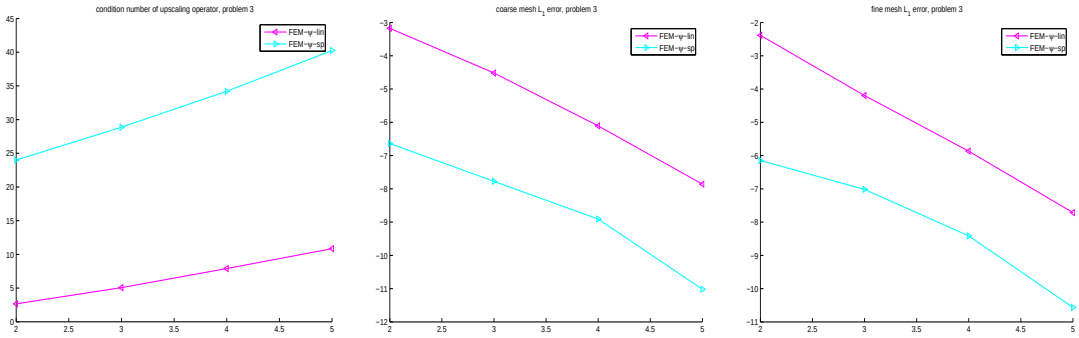

(a) *Condition Number.* **(b) *Coarse Mesh* L^1 *error.*** **(c) *Fine Mesh* L^1 *error.***

Figure 22: Example 3. Random Fourier Modes.

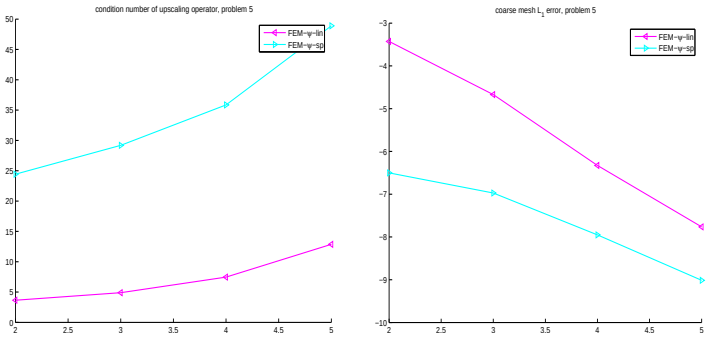

(a) *Condition Number.* **(b) *Coarse Mesh* L^1 *error.***

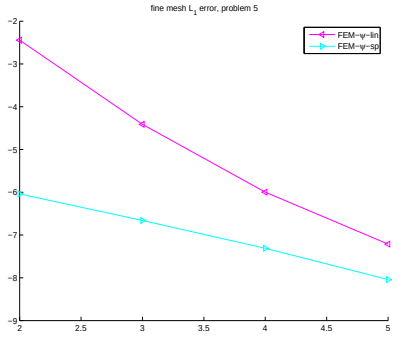

(c) *Fine Mesh* L^1 *error.*

Figure 23: Example 5. Percolation at criticality.

Acknowledgments. Part of the work of the first author has been supported by CNRS. The authors would like to thank Jean-Michel Roquejoffre for indicating us the correct references on nonlinear PDEs, Mathieu Desbrun for enlightening discussions on discrete exterior calculus [58] (a powerful tool that has put into evidence the intrinsic way to define discrete differential operators on irregular triangulations), Tom Hou and Jerry Marsden for stimulating discussions on multi-scale computation, Clothilde Melot and Stéphane Jaffard for stimulating discussions on multi-fractal analysis. Thanks are also due to Lexing Ying and Laurent Demanet for useful comments on the manuscript and G. Ben Arous for indicating us reference [72]. Many thanks are also due to Stefan Müller (MPI, Leipzig) for valuable suggestions and for indicating us the Hierarchical Matrices methods. We would like also to thank G. Allaire, F. Murat and S.R.S. Varadhan for stimulating discussions at the CIRM workshop on random homogenization and P. Schröder for stimulating discussions on splines based methods. We also thank an anonymous referee for detailed comments and suggestions.

References

[1] Giovanni Alessandrini and Vincenzo Nesi. Univalent σ-harmonic mappings: connections with quasiconformal mappings. *J. Anal. Math.*, 90:197–215, 2003.

[2] G. Allaire and R. Brizzi. A multi-scale finite element method for numerical homogenization. Technical report, CMAPX, 2004.

[3] B. Alpert, G. Beylkin, R. Coifman, and V. Rokhlin. Wavelet-like bases for the fast solution of second-kind integral equations. *SIAM J. Sci. Comput.*, 14(1):159–184, 1993.

[4] Alano Ancona. Some results and examples about the behavior of harmonic functions and Green's functions with respect to second order elliptic operators. *Nagoya Math. J.*, 165:123–158, 2002.

[5] Antonios Armaou, Constantinos I. Siettos, and Ioannis G. Kevrekidis. Time-steppers and 'coarse' control of distributed microscopic processes. *Internat. J. Robust Nonlinear Control*, 14(2):89–111, 2004. Control of complex process systems.

[6] Kari Astala and Vincenzo Nesi. Composites and quasiconformal mappings: new optimal bounds in two dimensions. *Calc. Var. Partial Differential Equations*, 18(4):335–355, 2003.

[7] Amir Averbuch, Gregory Beylkin, Ronald Coifman, and Moshe Israeli. Multiscale inversion of elliptic operators. In *Signal and image representation in combined spaces*, volume 7 of *Wavelet Anal. Appl.*, pages 341–359. Academic Press, San Diego, CA, 1998.

[8] M.T. Barlow, T. Coulhon, and T. Kumagai. Characterization of sub-gaussian heat kernel estimates on strongly recurrent graphs. 2005. To appear Comm. Pure Appl. Math.

[9] M. Bebendorf and Y. Chen. Efficient solution of nonlinear elliptic problems using hierarchical matrices with broyden updates. *preprint 51/2005, Max-Planck-Institut MiS, Leipzig*, 2005.

[10] Mario Bebendorf. Approximate inverse preconditioning of fe systems for elliptic operators with non-smooth coefficients. *Preprint 7/2004, Max-Planck-Institute MiS, Leipzig*, 2005.

[11] Mario Bebendorf. Efficient inversion of galerkin matrices of general second-order elliptic differential operators with nonsmooth coefficients. *Math. Comp.*, 74:1179–1199, 2005.

[12] Mario Bebendorf. Why approximate lu decompositions of finite element discretizations of elliptic operators can be computed with almost linear complexity. *Preprint 8/2005, Max-Planck-Institute MiS, Leipzig*, 2005.

[13] Mario Bebendorf and Wolfgang Hackbusch. Existence of $\mathcal{H}$-matrix approximants to the inverse FE-matrix of elliptic operators with L^∞-coefficients. *Numer. Math.*, 95(1):1–28, 2003.

[14] Gérard Ben Arous and Houman Owhadi. Multiscale homogenization with bounded ratios and anomalous slow diffusion. *Comm. Pure Appl. Math.*, 56(1):80–113, 2003.

[15] A. Bensoussan, J. L. Lions, and G. Papanicolaou. *Asymptotic analysis for periodic structure*. North Holland, Amsterdam, 1978.

[16] G. Beylkin, R. Coifman, and V. Rokhlin. Fast wavelet transforms and numerical algorithms. I. *Comm. Pure Appl. Math.*, 44(2):141–183, 1991.

[17] G. Beylkin, R. Coifman, and V. Rokhlin. Fast wavelet transforms and numerical algorithms. I. In *Wavelets and applications (Marseille, 1989)*, volume 20 of *RMA Res. Notes Appl. Math.*, pages 368–393. Masson, Paris, 1992.

[18] Gregory Beylkin and Nicholas Coult. A multiresolution strategy for reduction of elliptic PDEs and eigenvalue problems. *Appl. Comput. Harmon. Anal.*, 5(2):129–155, 1998.

[19] M. E. Brewster and G. Beylkin. A multiresolution strategy for numerical homogenization. *Appl. Comput. Harmon. Anal.*, 2(4):327–349, 1995.

[20] Franco Brezzi and Donatella Marini. Subgrid phenomena and numerical schemes. In *Frontiers in numerical analysis (Durham, 2002)*, Universitext, pages 1–16. Springer, Berlin, 2003.

[21] Marc Briane, Graeme W. Milton, and Vincenzo Nesi. Change of sign of the corrector's determinant for homogenization in three-dimensional conductivity. *Arch. Ration. Mech. Anal.*, 173(1):133–150, 2004.

[22] S. Campanato. Un risultato relativo ad equazioni ellittiche del secondo ordine di tipo non variazionale. *Ann. Scuola Norm. Sup. Pisa (3)*, 21:701–707, 1967.

[23] A. Chertock and D. Levy. On wavelet-based numerical homogenization. *Multiscale Modeling and Simulation*, 3:65–88, 2004.

[24] F. Cirak, M. ORTIZ, and P. Schröder. Subdivision surfaces: A new paradigm for thin-shell finite-element analysis. *Internat. J. Numer. Methods Eng.*

[25] R. Coifman, P.-L. Lions, Y. Meyer, and S. Semmes. Compensated compactness and Hardy spaces. *J. Math. Pures Appl. (9)*, 72(3):247–286, 1993.

[26] Ennio De Giorgi. Sulla differenziabilità e l'analiticità delle estremali degli integrali multipli regolari. *Mem. Accad. Sci. Torino. Cl. Sci. Fis. Mat. Nat. (3)*, 3:25–43, 1957.

[27] J. Dolbow, M. A. Khaleel, and J. Mitchell. Multiscale mathematics initiative: A roadmap. Technical report, DOE, 2004. Prepared for the U.S. Department of Energy under Contract DE-AC05-76RL01830.

[28] Mihai Dorobantu and Björn Engquist. Wavelet-based numerical homogenization. *SIAM J. Numer. Anal.*, 35(2):540–559 (electronic), 1998.

[29] W. E, B. Engquist, X. Li, W. Ren, and E. Vanden-Eijnden. The heterogeneous multiscale method: A review. Technical report, preprint. http://www.math.princeton.edu/multiscale/review.pdf.

[30] Yalchin R. Efendiev, Thomas Y. Hou, and Xiao-Hui Wu. Convergence of a nonconforming multiscale finite element method. *SIAM J. Numer. Anal.*, 37(3):888–910 (electronic), 2000.

[31] R.S. Ellis. *Entropy, Large deviations, and Statistical Mechanics.* Springer, 1985.

[32] A. Ern and J.-L. Guermond. *Theory and practice of finite element methods.*, volume 159 of *Applied Mathematical Sciences*. Springer, 2004. Two volumes bound as one.

[33] Charbel Farhat, Isaac Harari, and Leopoldo P. Franca. The discontinuous enrichment method. *Comput. Methods Appl. Mech. Engrg.*, 190(48):6455–6479, 2001.

[34] Charbel Farhat, Isaac Harari, and Ulrich Hetmaniuk. The discontinuous enrichment method for multiscale analysis. *Comput. Methods Appl. Mech. Engrg.*, 192(28-30):3195–3209, 2003. Multiscale computational mechanics for materials and structures (Cachan, 2002).

[35] M. Fenn and G. Steidl. Fmm and $\mathcal{H}$-matrices: a short introduction to the basic idea. Technical report, Department for Mathematics and Computer Science, University of Mannheim ; TR-2002-008, 2004.

[36] Jacob Fish and Amir Wagiman. Multiscale finite element method for a locally nonperiodic heterogeneous medium. *Comput. Mech.*, 12(3):164–180, 1993.

[37] Jacob Fish and Yuan Zheng. Multi-scale enrichment based on partition of unity. *Int. J. Num. Meth. Engng*, 2005.

[38] U. Freiberg and M. Zähle. Harmonic calculus on fractals—a measure geometric approach. I. *Potential Anal.*, 16(3):265–277, 2002.

[39] Uta Freiberg. Analytical properties of measure geometric Krein-Feller-operators on the real line. *Math. Nachr.*, 260:34–47, 2003.

[40] U. Frisch and G. Parisi. Fully developed turbulence and intermittency. In *Proceedings of the International School in Physics, "E.Fermi", Course. Turbulence and Predictability in Geophysical Fluid Dynamics and Climate Dynamics*, page 2184. North Holland Amsterdam, 1985.

[41] A. C. Gilbert. A comparison of multiresolution and classical one-dimensional homogenization schemes. *Appl. Comput. Harmon. Anal.*, 5(1):1–35, 1998.

[42] Olivier Goubet. Séparation des variables dans le problème de Stokes. Application à son approximation multiéchelles éléments finis. *C. R. Acad. Sci. Paris Sér. I Math.*, 315(12):1315–1318, 1992.

[43] L. Greengard and V. Rokhlin. A fast algorithm for particle simulations. *J. Comput. Phys.*, 73(2):325–348, 1987.

[44] W. Hackbusch. On the multigrid method applied to difference equations. *Computing*, 20(4):291–306, 1978.

[45] Wolfgang Hackbusch, Lars Grasedyck, and Steffen Börm. An introduction to hierarchical matrices. In *Proceedings of EQUADIFF, 10 (Prague, 2001)*, volume 127, pages 229–241, 2002.

[46] Viet Ha Hoang and Christoph Schwab. High-dimensional finite elements for elliptic problems with multiple scales. *Multiscale Model. Simul.*, 3(1):168–194 (electronic), 2004/05.

[47] Klaus Höllig. *Finite element methods with B-splines*, volume 26 of *Frontiers in Applied Mathematics*. Society for Industrial and Applied Mathematics (SIAM), Philadelphia, PA, 2003.

[48] Klaus Höllig, Ulrich Reif, and Joachim Wipper. Weighted extended B-spline approximation of Dirichlet problems. *SIAM J. Numer. Anal.*, 39(2):442–462 (electronic), 2001.

[49] Thomas Y. Hou and Xiao-Hui Wu. A multiscale finite element method for elliptic problems in composite materials and porous media. *J. Comput. Phys.*, 134(1):169–189, 1997.

[50] Thomas Y. Hou, Xiao-Hui Wu, and Yu Zhang. Removing the cell resonance error in the multiscale finite element method via a Petrov-Galerkin formulation. *Commun. Math. Sci.*, 2(2):185–205, 2004.

[51] Stéphane Jaffard. Formalisme multifractal pour les fonctions. *C. R. Acad. Sci. Paris Sér. I Math.*, 317(8):745–750, 1993.

[52] V. V. Jikov, S. M. Kozlov, and O. A. Oleinik. *Homogenization of Differential Operators and Integral Functionals*. Springer-Verlag, 1991.

[53] Jun Kigami. Harmonic calculus on limits of networks and its application to dendrites. *J. Funct. Anal.*, 128(1):48–86, 1995.

[54] S. H. Lee, P. Jenny, and H. A. Tchelepi. Multi-scale finite-volume method for elliptic problems in subsurface flow simulation. *Journal of Computational Physics*, 187:47–67, 2003.

[55] S. Leonardi. Weighted Miranda-Talenti inequality and applications to equations with discontinuous coefficients. *Comment. Math. Univ. Carolin.*, 43(1):43–59, 2002.

[56] A. Maugeri, D. K. Palagachev, and L. G. Softova. *Elliptic and Parabolic Equations with Discontinuous Coefficients*, volume 109 of *Mathematical Research*. Wiley-VCH, 2000.

[57] Clothilde Mélot. *Sur les singularités oscillantes et les formalsime multifractal*. PhD thesis, University of Paris XII, 2002.

[58] Mark Meyer, Mathieu Desbrun, Peter Schröder, and Alan H. Barr. Discrete differential-geometry operators for triangulated 2-manifolds. In *Visualization and mathematics III*, Math. Vis., pages 35–57. Springer, Berlin, 2003.

[59] Jürgen Moser. On Harnack's theorem for elliptic differential equations. *Comm. Pure Appl. Math.*, 14:577–591, 1961.

[60] François Murat. Compacité par compensation. *Ann. Scuola Norm. Sup. Pisa Cl. Sci. (4)*, 5(3):489–507, 1978.

[61] François Murat and Luc Tartar. H-convergence. In *Topics in the mathematical modelling of composite materials*, volume 31 of *Progr. Nonlinear Differential Equations Appl.*, pages 21–43. Birkhäuser Boston, Boston, MA, 1997.

[62] Boaz Nadler, Stephane Lafon, Ronald R. Coifman, and Ioannis G. Kevrekidis. Diffusion maps, spectral clustering and reaction coordinates of dynamical systems. *Arxiv math.NA/0503445*, 2005.

[63] J. Nash. Continuity of solutions of parabolic and elliptic equations. *Amer. J. Math.*, 80:931–954, 1958.

[64] Assad A. Oberai and Peter M. Pinsky. A multiscale finite element method for the Helmholtz equation. *Comput. Methods Appl. Mech. Engrg.*, 154(3-4):281–297, 1998.

[65] H. Owhadi and L. Zhang. Homogenization of parabolic equations with a continuum of space and time scales. 2005. preprint.

[66] Houman Owhadi. Anomalous slow diffusion from perpetual homogenization. *Ann. Probab.*, 31(4):1935–1969, 2003.

[67] Houman Owhadi. Averaging versus chaos in turbulent transport? *Comm. Math. Phys.*, 247(3):553–599, 2004.

[68] R. H. Riedi. An introduction to multifractals. Technical report, Rice University, 1997. available at http://www.stat.rice.edu∼riedi/.

[69] V. B. Shenoy, R. Miller, E. B. Tadmor, D. Rodney, R. Phillips, and M. Ortiz. An adaptive finite element approach to atomic-scale mechanics—the quasicontinuum method. *J. Mech. Phys. Solids*, 47(3):611–642, 1999.

[70] Leon Simon. Global estimates of Hölder continuity for a class of divergence-form elliptic equations. *Arch. Rational Mech. Anal.*, 56:253–272, 1974.

[71] Robert S. Strichartz. Function spaces on fractals. *J. Funct. Anal.*, 198(1):43–83, 2003.

[72] Daniel W. Stroock and Weian Zheng. Markov chain approximations to symmetric diffusions. *Ann. Inst. H. Poincaré Probab. Statist.*, 33(5):619–649, 1997.

[73] L. Tartar. Compensated compactness and applications to partial differential equations. In *Nonlinear analysis and mechanics: Heriot-Watt Symposium, Vol. IV*, volume 39 of *Res. Notes in Math.*, pages 136–212. Pitman, Boston, Mass., 1979.

[74] L. Tartar. Homogénéisation et compacité par compensation. In *Séminaire Goulaouic-Schwartz (1978/1979)*, pages Exp. No. 9, 9. École Polytech., Palaiseau, 1979.

[75] W. L. Wan, Tony F. Chan, and Barry Smith. An energy-minimizing interpolation for robust multigrid methods. *SIAM J. Sci. Comput.*, 21(4):1632–1649 (electronic), 1999/00.

[76] Michel Zinsmeister. *Thermodynamic formalism and holomorphic dynamical systems*, volume 2 of *SMF/AMS Texts and Monographs*. American Mathematical Society, Providence, RI, 2000. Translated from the 1996 French original by C. Greg Anderson.